On the structure and stability of magnetic tower jets and the formation of disks in binaries

Martín Huarte-Espinosa, Adam Frank, Eric Blackman, Jonathan Carroll-Nellenback, Jason Nordhaus (Uni. of Rochester, New York), Andrea Ciardi (LERMA, Paris), Patrick Hartigan (Rice Uni, Texas), Sergey Lebedev and Jeremy Chittenden (Imperial College London)

Seminario del IA-UNAM, 22 Ago 2012

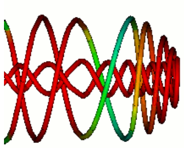

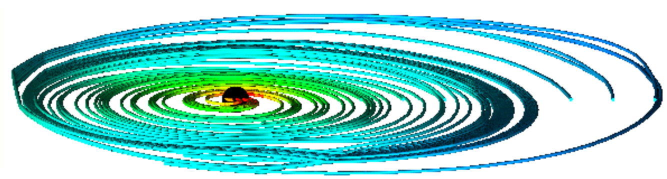

instituto de astronomía

unam

Motivation

Lebedev et al.

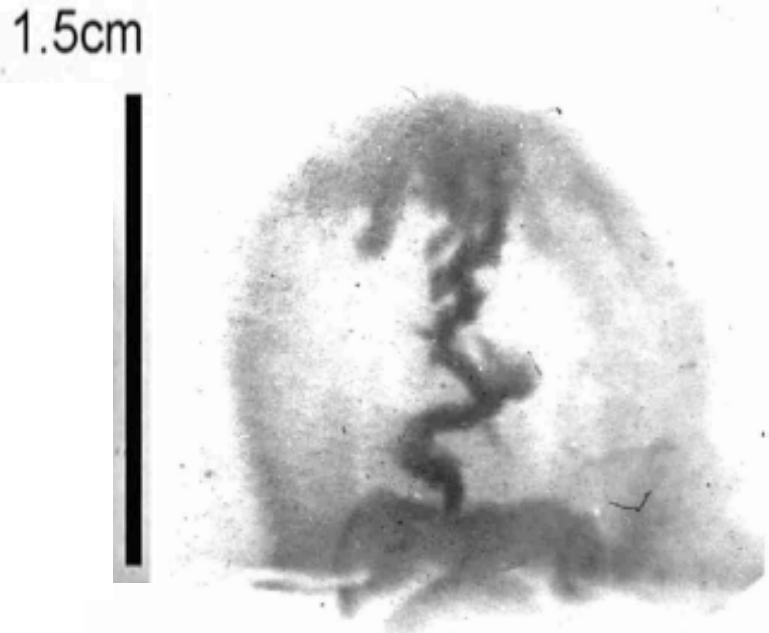

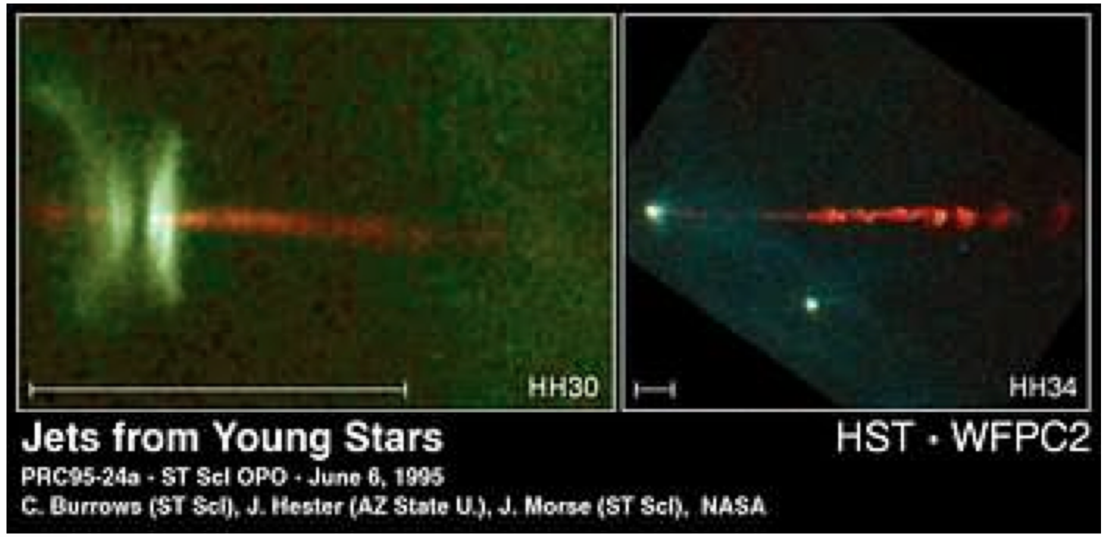

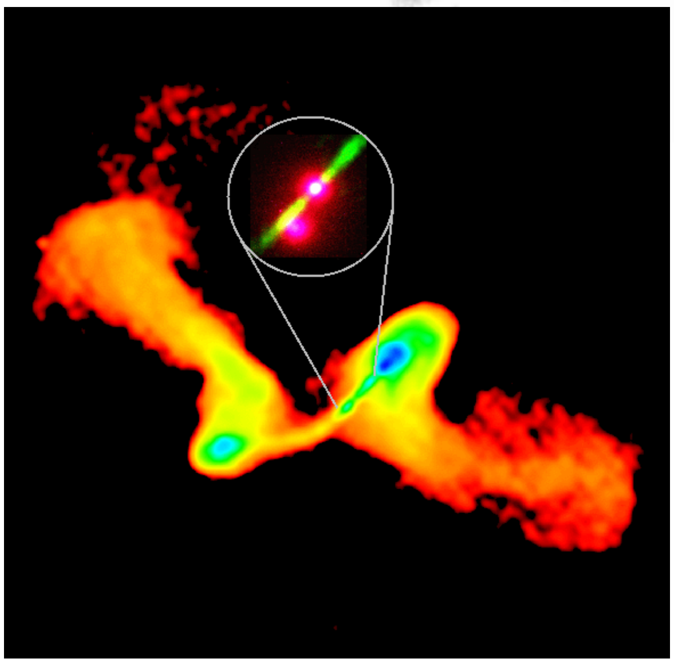

^ NGC 326, Murgia et al.

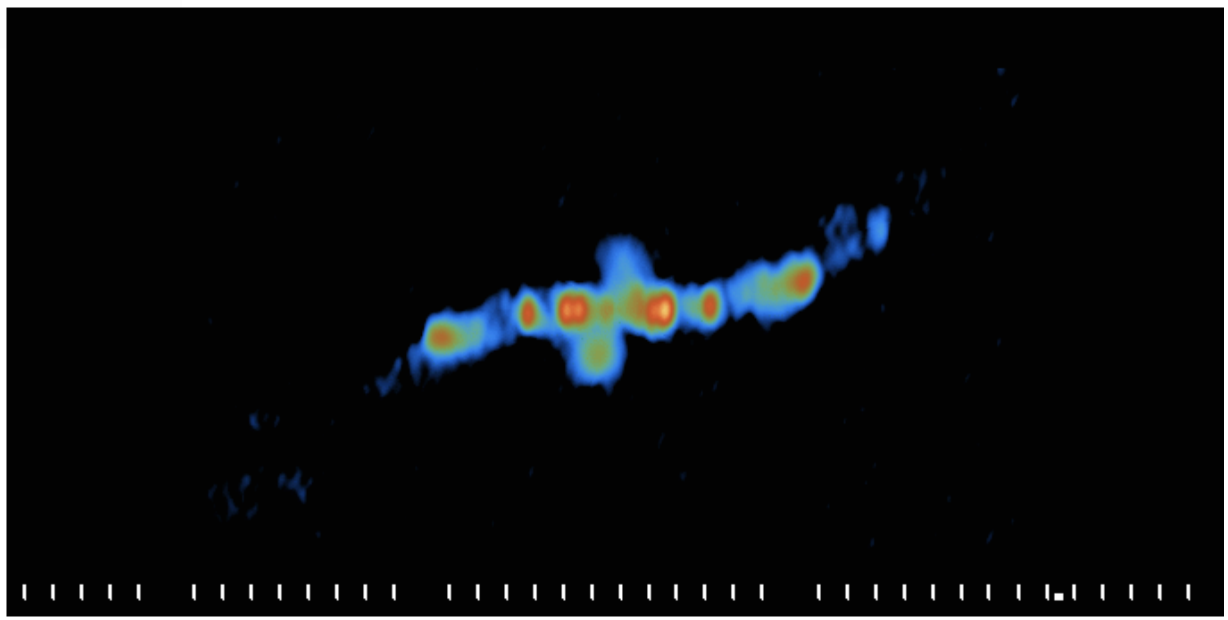

Q (**X**,t) = Magnetic flux / kinetic-energy flux ?

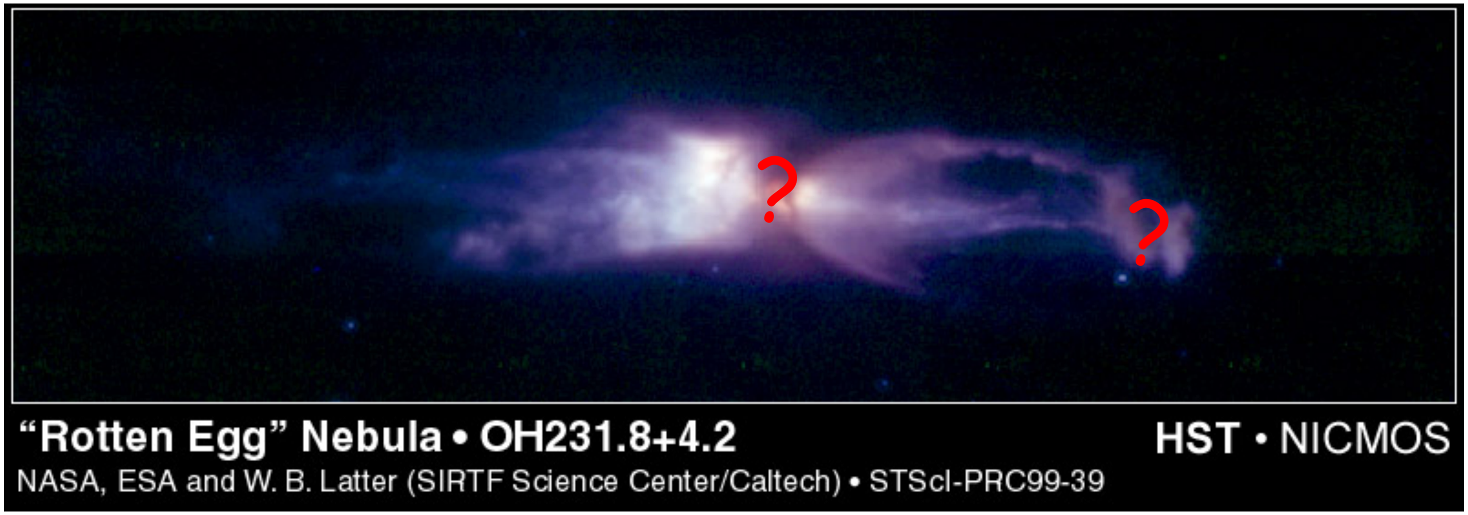

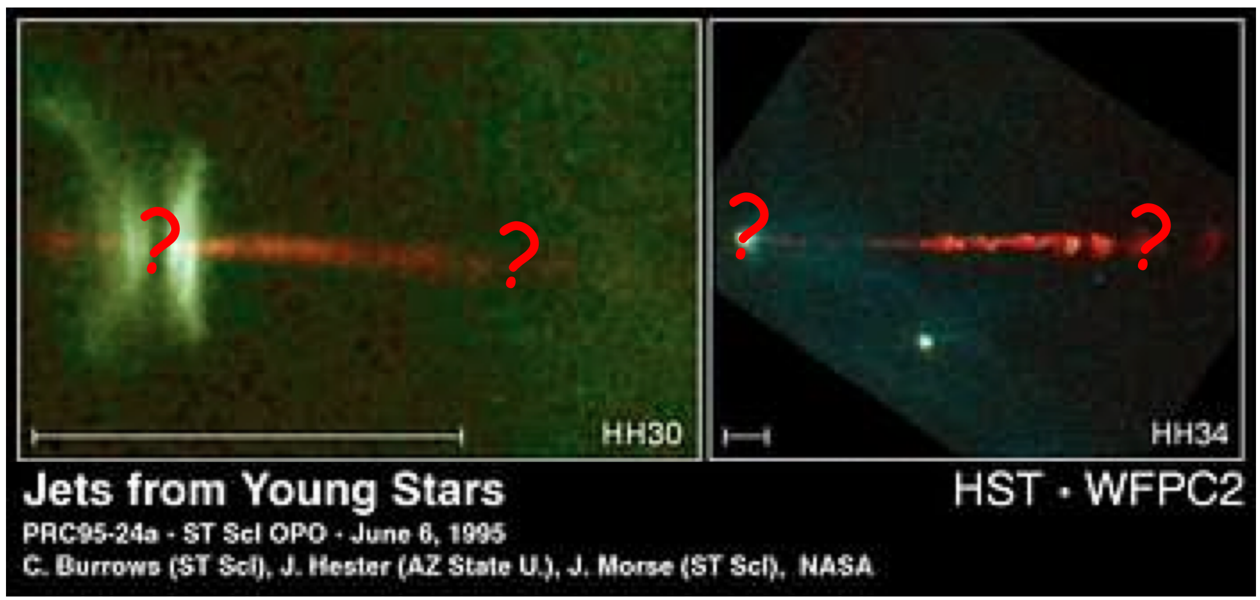

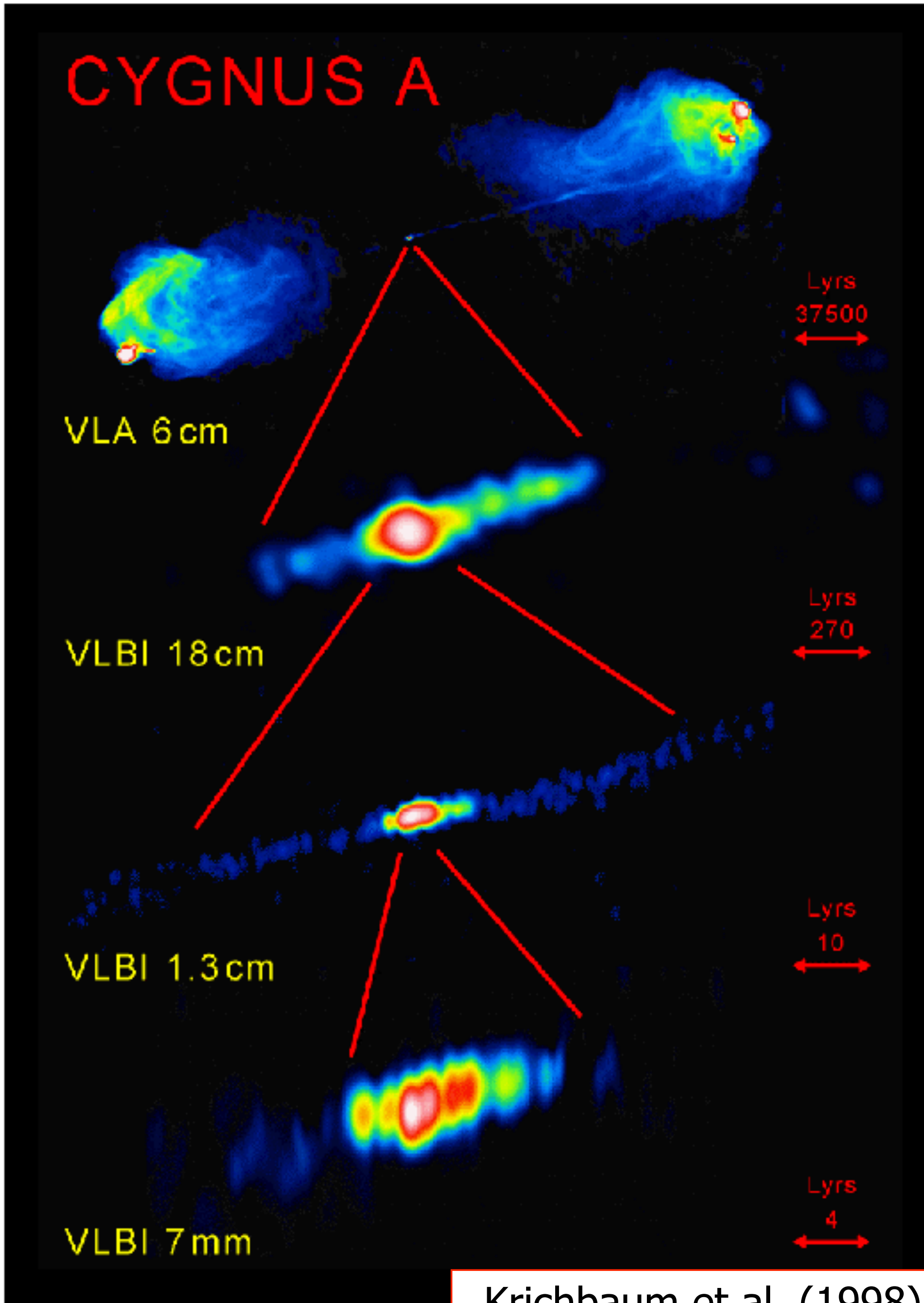

Krichbaum et al. (1998)

$|\mathbf{B}|_{weak}$

$|\mathbf{B}|_{weak}$

$|\mathbf{B}|_{?}$

$|\mathbf{B}|_{strong}$

Outline

1. Types of magnetized jets
2. Laboratory experiment jets
3. Simulations of magnetic towers,
4. New results on disks formed in common envelope binaries
5. Summary and discussion

Jet l~~a~~unch

Ingredients:
-1 **compact object**
-some **accreted** plasma
-some **magnetic fields**

Preparation:
Stir (**rotation**) vigorously until a hot disk is formed and the magnetic fields are helical & strong
Enjoy!

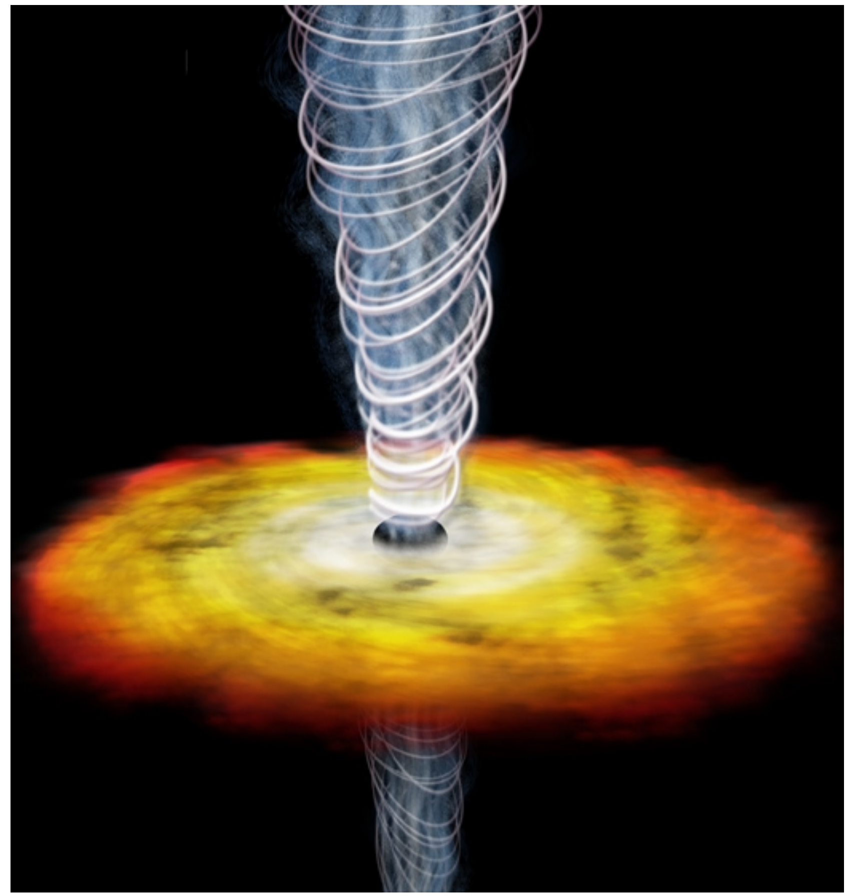

Magnetocentrifugal jets (Blandford & Payne 1982; Ouyed & Pudritz 1997; Ustyugova et al. 1999; Blackman et al. 2001)

→ *magnetic fields only dominate out to the Alfvén radius*

Poynting flux dominated jets (**PFD**; Lynden-Bell 1996; Ustyugova et al. ‘00; Li et al. ‘01; Lovelace et al. ‘02; Nakamura & Meier ‘04)

→ *magnetic fields dominate the jet structure*

Laboratory experiments

PFD jets, or magnetic towers, produced in a MAGPIE generator at Imperial College London. 1MA pulse current flows radially through 16 x 13μm tungsten metallic wires a central electrode. ~1 MG toroidal magnetic field produced below the wires (Lebedev et al., 2005).

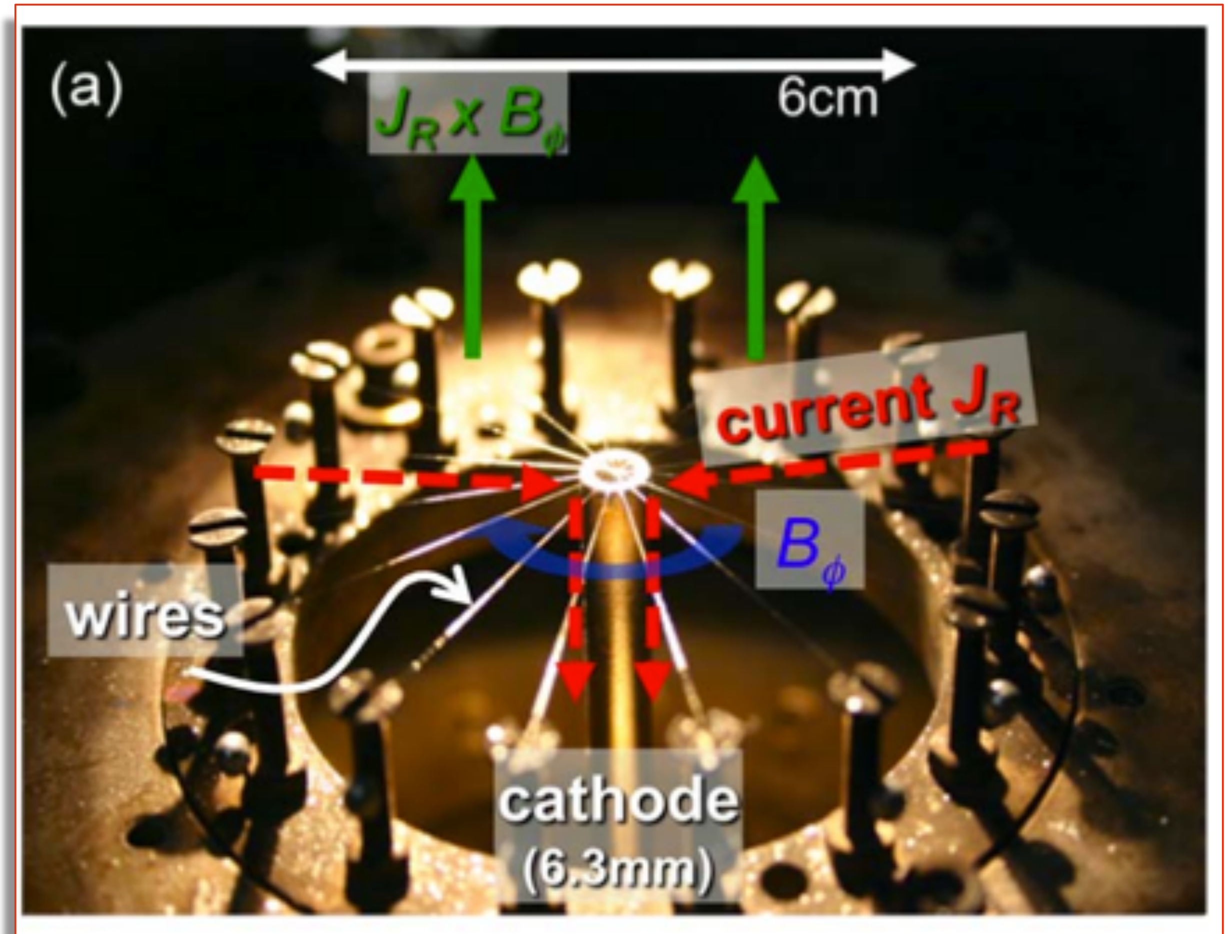

Evolution with XUV

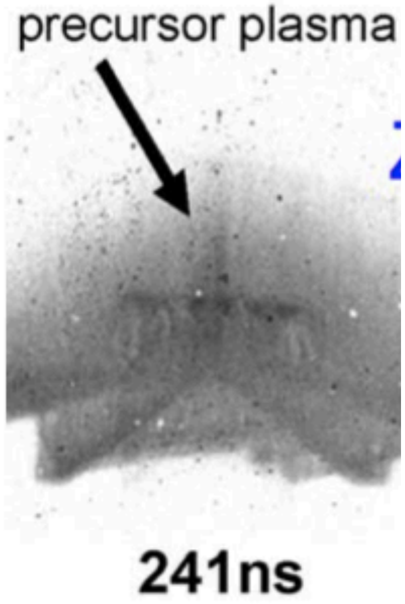

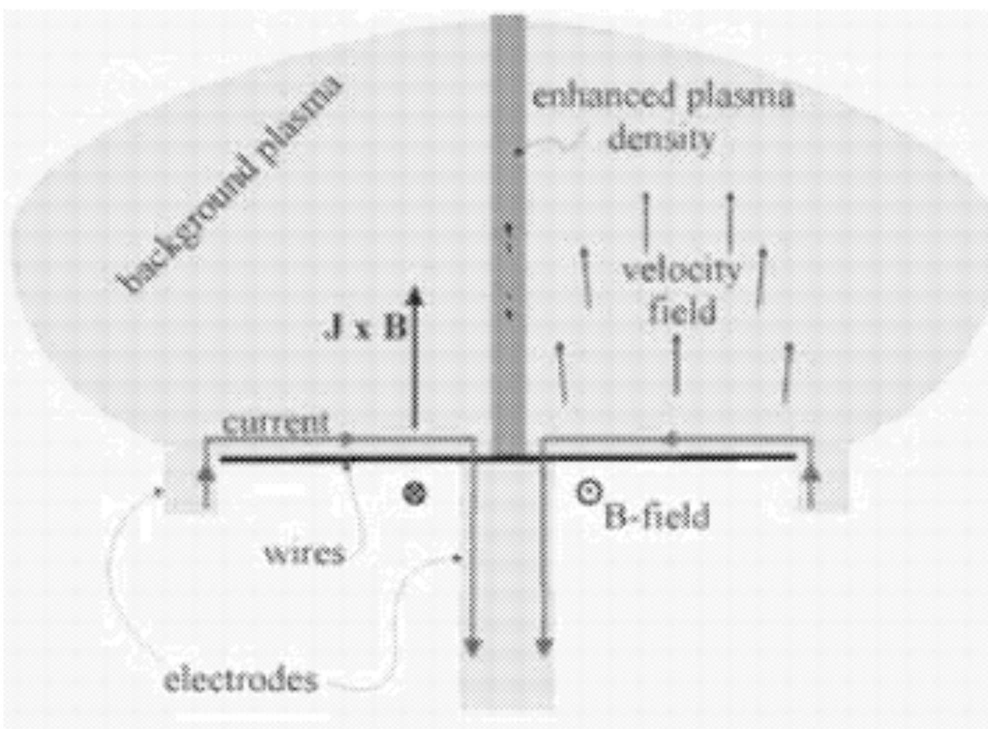

wire ablation + JxB force produce background plasma

resistive diffusion keeps current close to wires

Lebedev et al. 2005
Suzuki-Vidal et al. 2010

Evolution with XUV

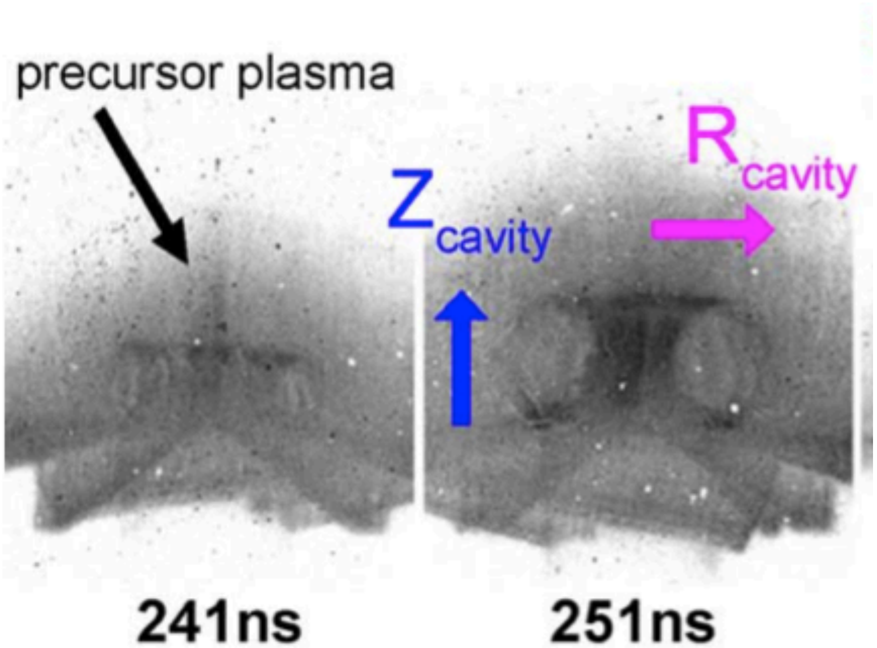

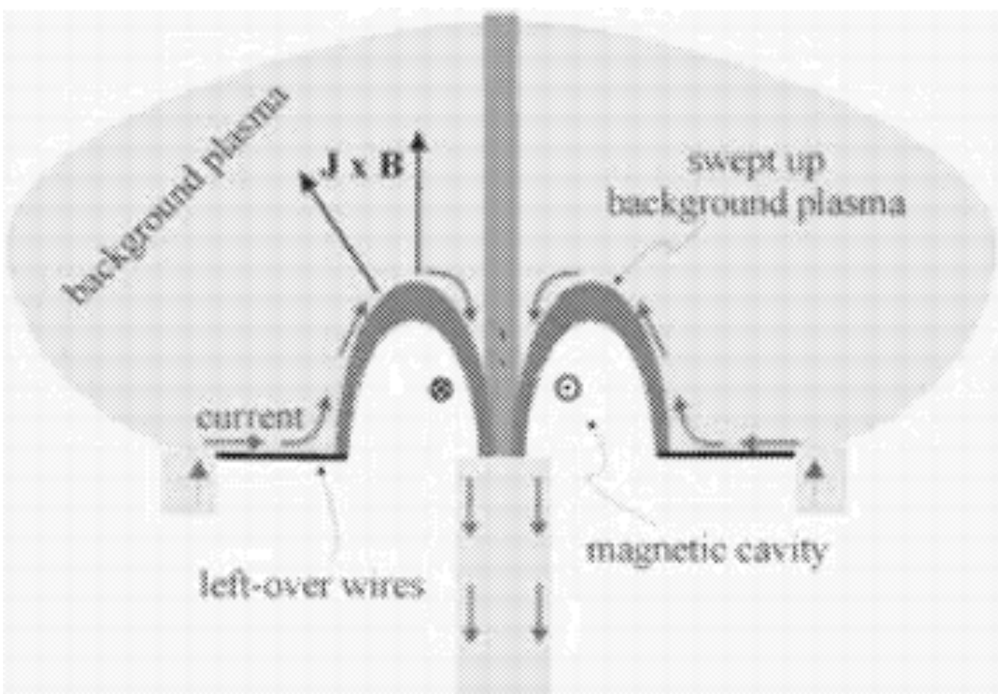

Full wire ablation near the central electrode forms a magnetic cavity.

Lebedev et al. 2005
Suzuki-Vidal et al. 2010

Evolution with XUV

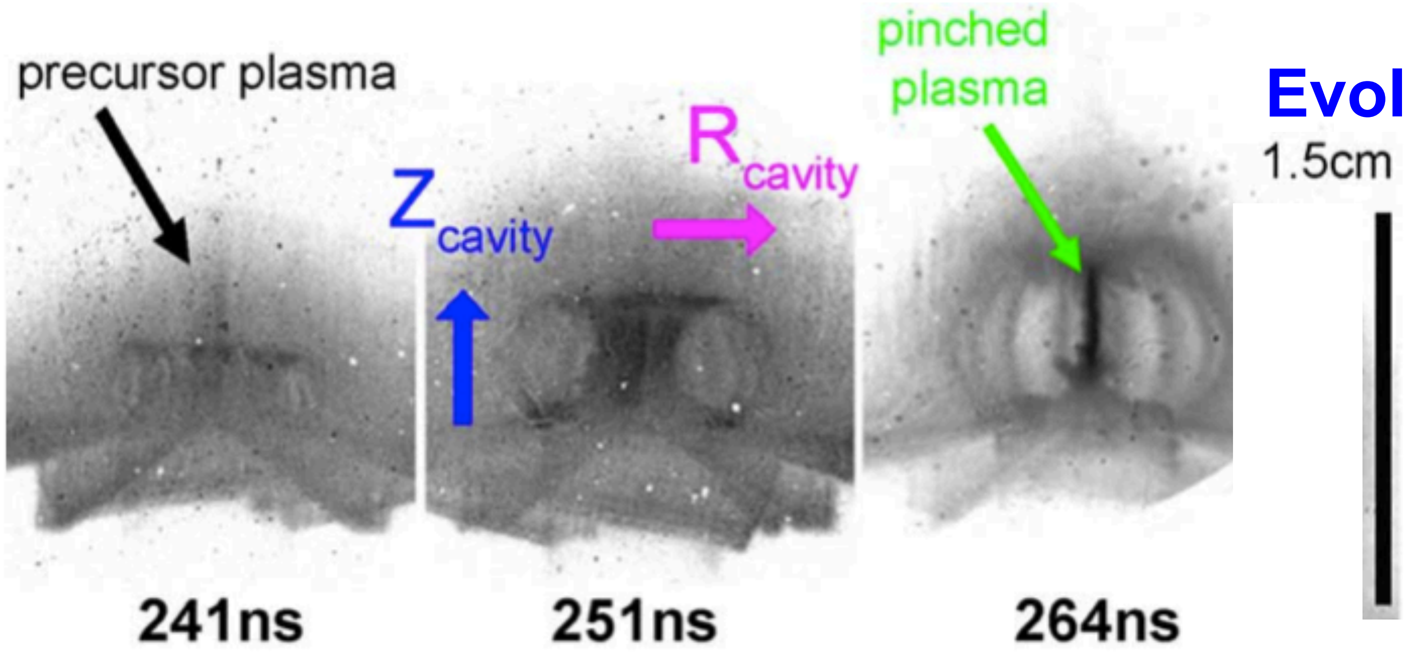

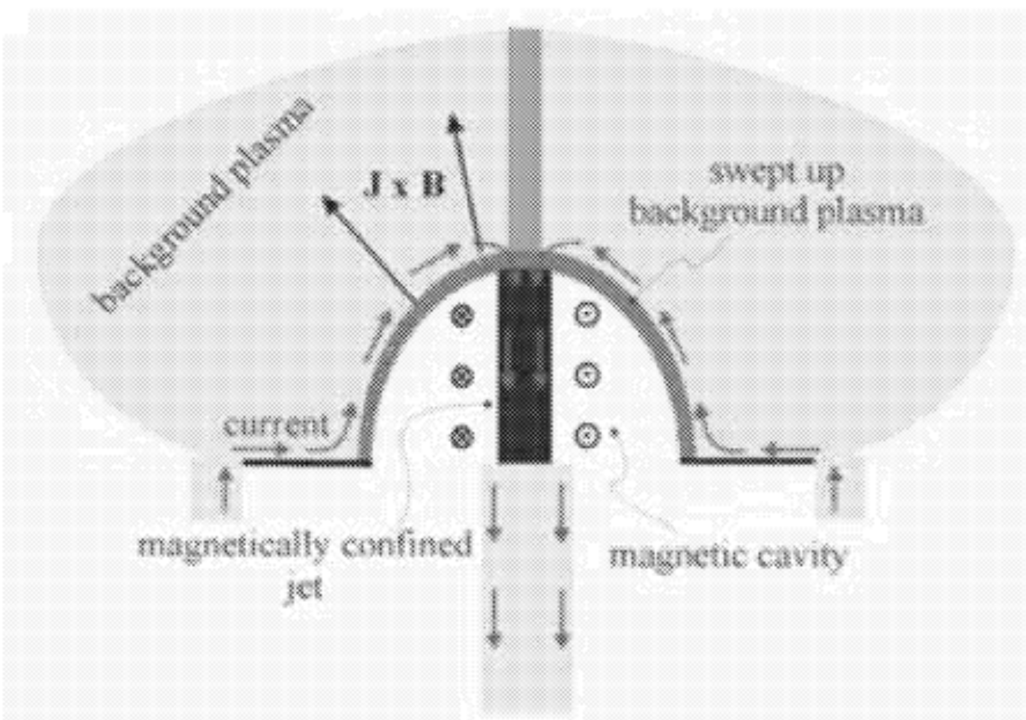

Expanding magnetic tower jet driven upwards by toroidal magnetic field pressure

Lebedev et al. 2005
Suzuki-Vidal et al. 2010

Evolution with XUV

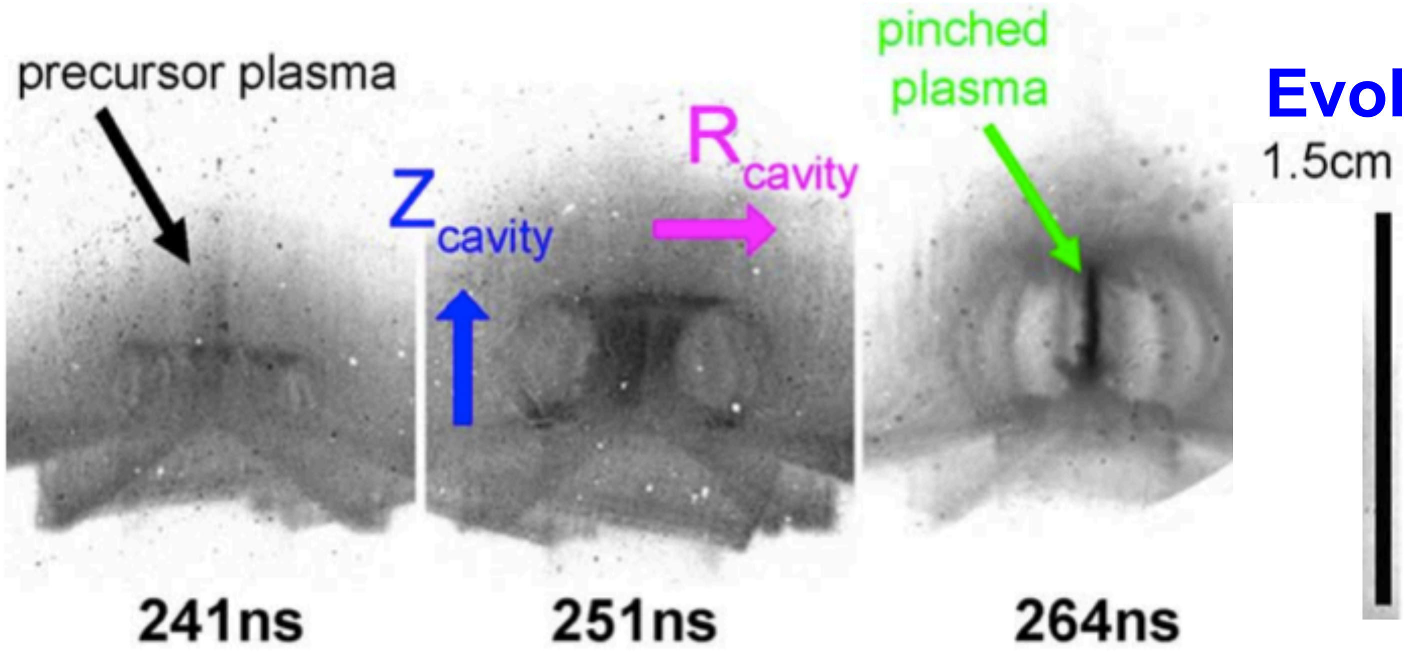

Jet *Collimation* by hoop stress

Magnetic bubble *Collimation* by ambient medium

Consistent with Lynden-Bell '96, '03

Once the jet forms

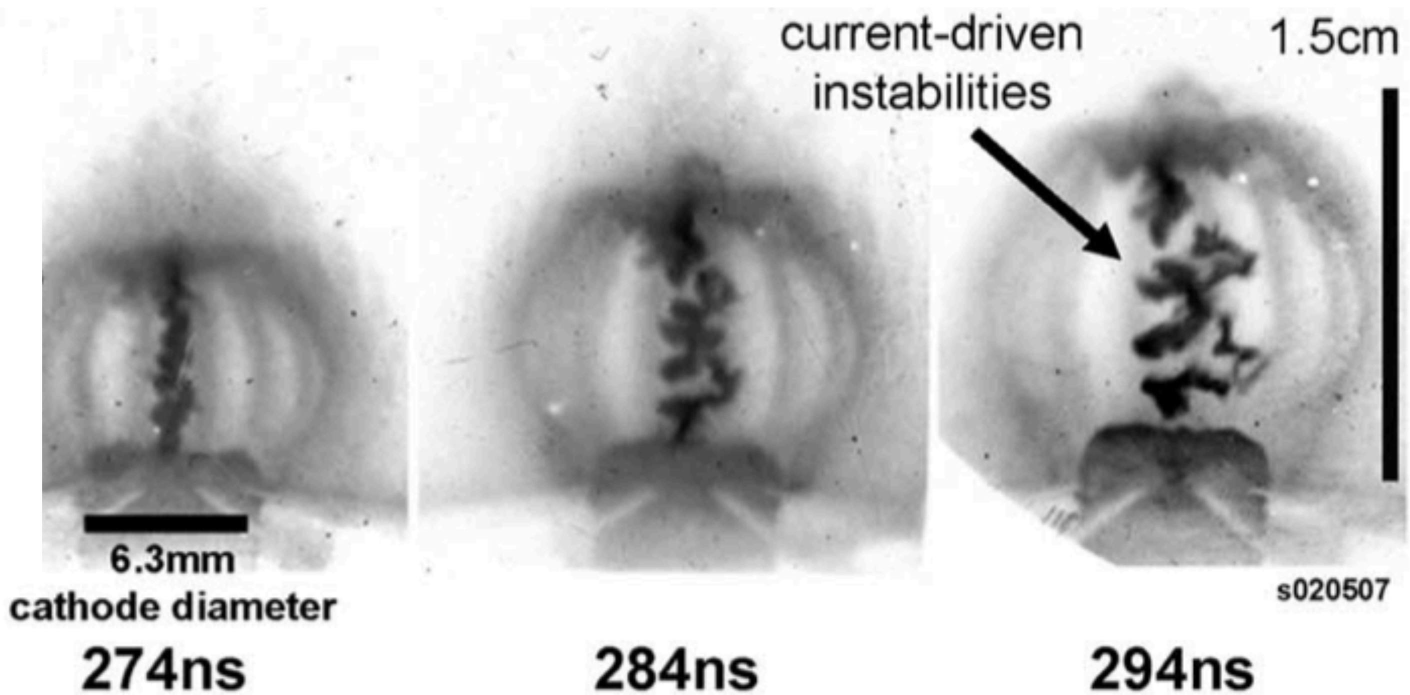

Lebedev et al. 2005
Suzuki-Vidal et al. 2010

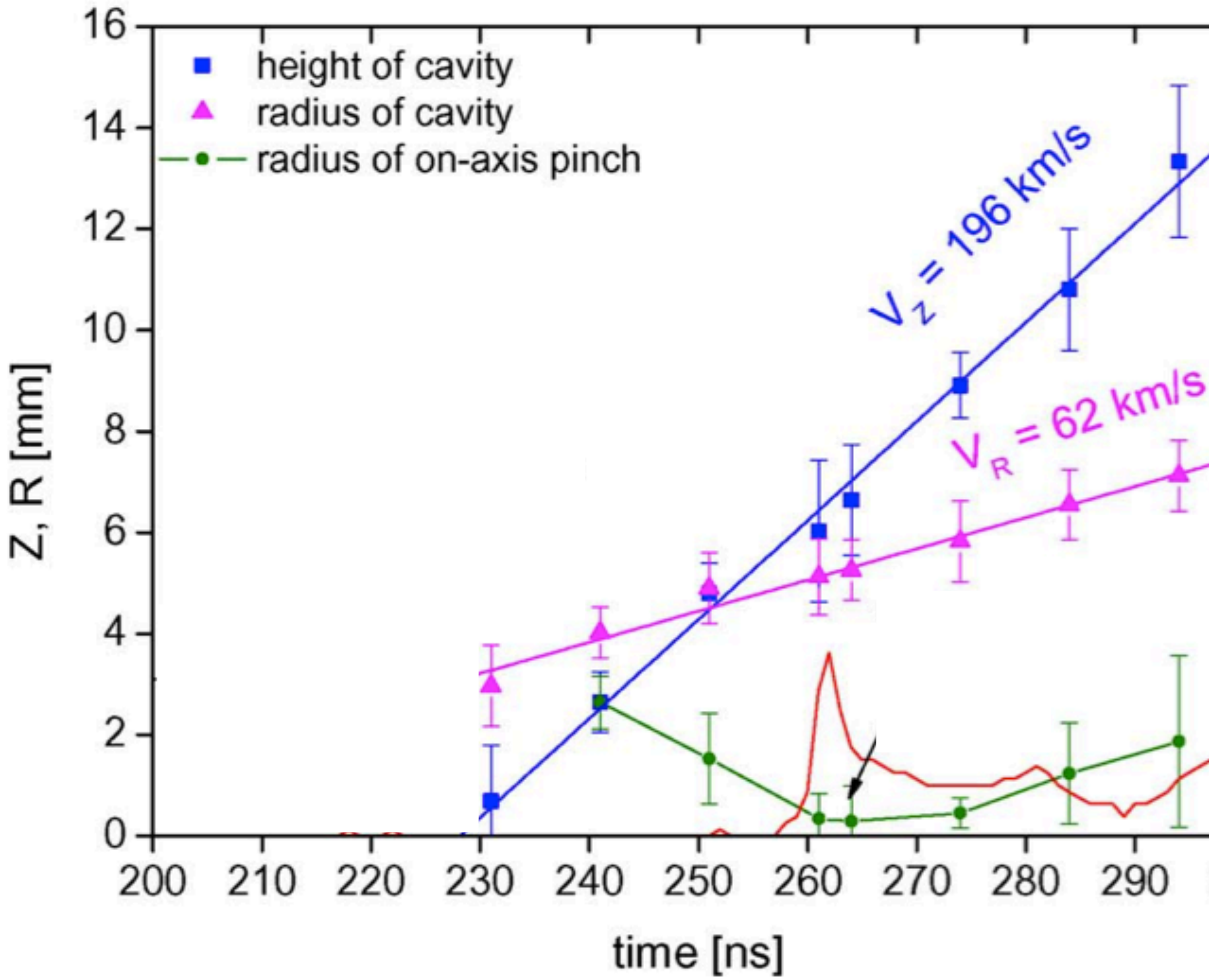

(Suzuki-Vidal et al. 2010)

Radial wire array (again) + B_{axial}

(a)

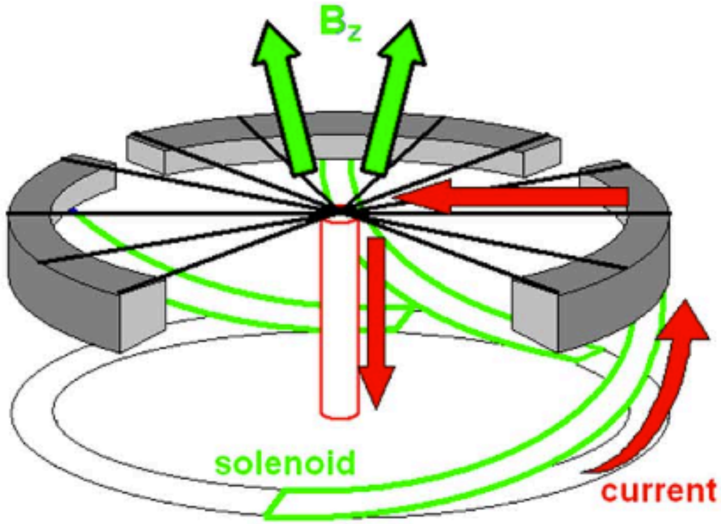

outer solenoid

(b)

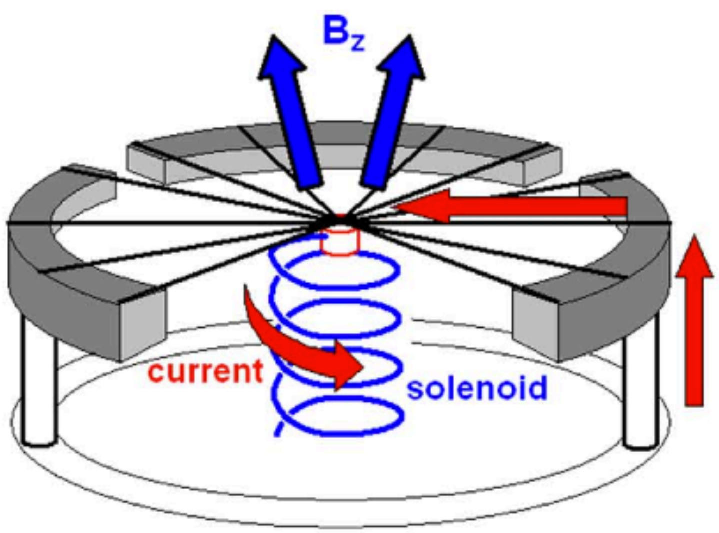

cathode solenoid

Suzuki-Vidal et al. 2011

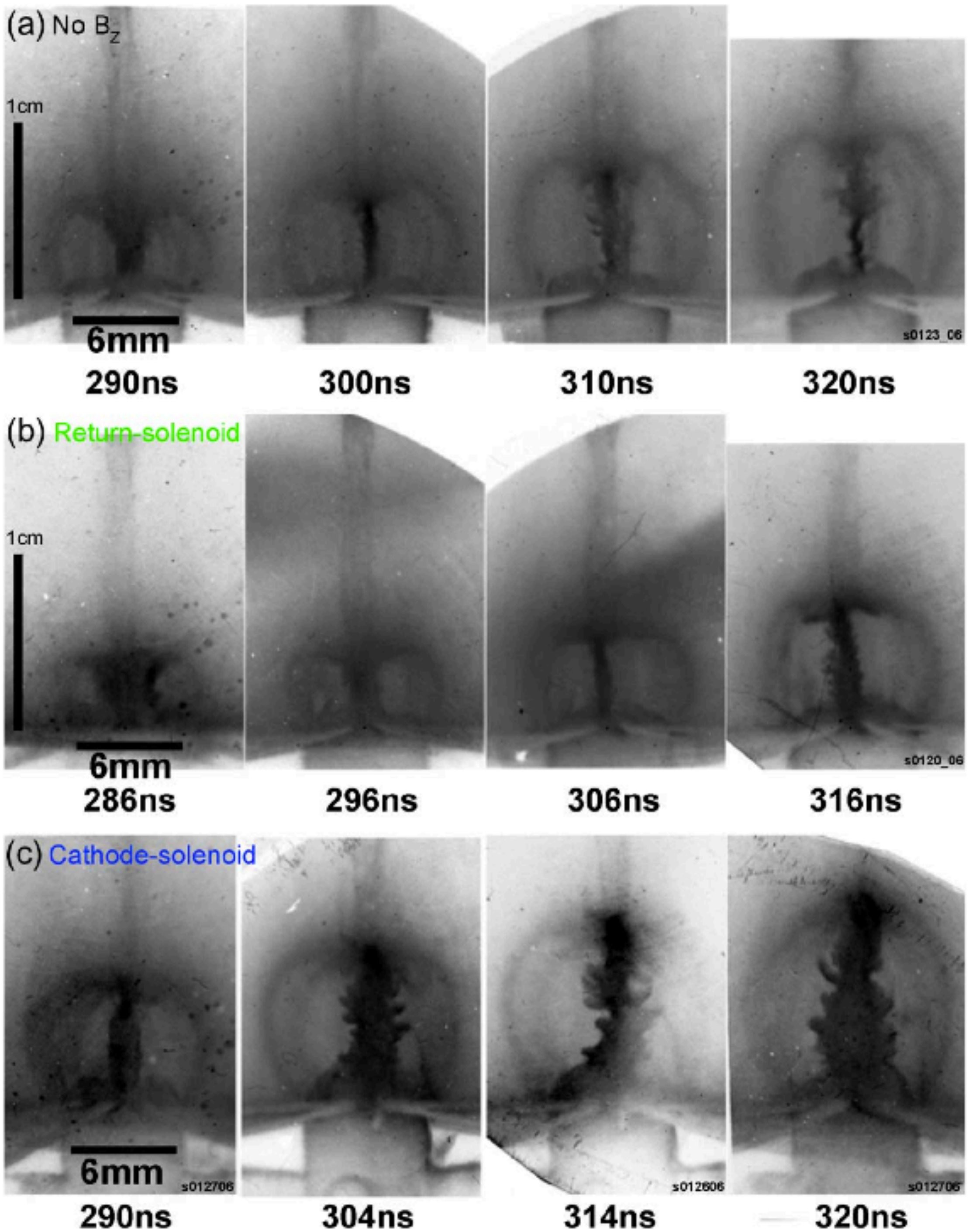

B_z affects axial compression

$B_z \propto R_{column}$

More stable

Suzuki-Vidal et al. '10

Simulations (Ciardi et al. 2007)

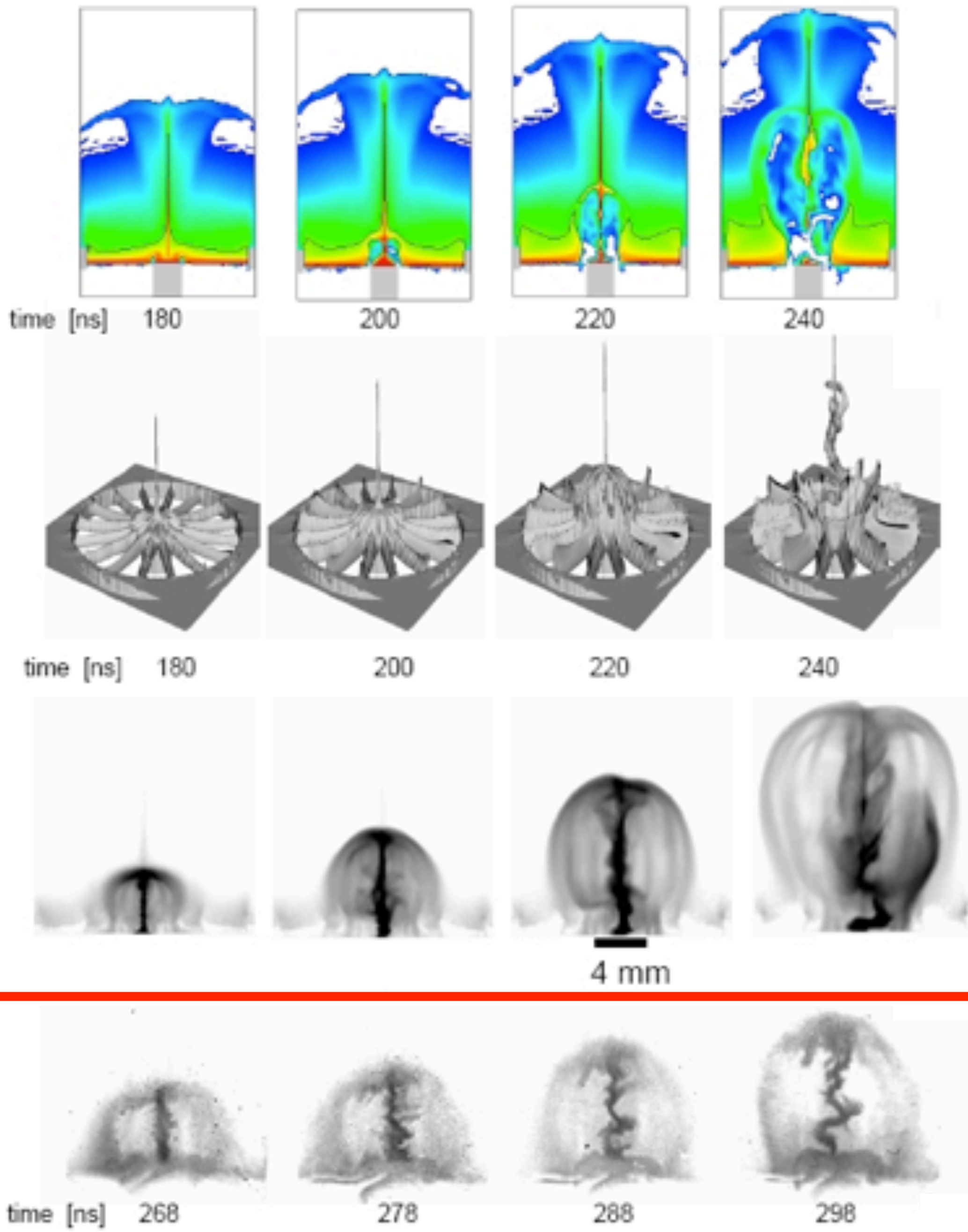

Density slices

Iso-density surfaces

Synthetic emission

XUV emission from **experiment** (again)

Out model: stellar magnetic towers

(Huarte-Espinosa et al. 2012, accepted in ApJ, arxiv:1204.0800)

THE ASTROPHYSICAL JOURNAL SUPPLEMENT SERIES, 182:519–542, 2009 June doi:10.1088/0067-0049/182/2/519

SIMULATING MAGNETOHYDRODYNAMICAL FLOW WITH CONSTRAINED TRANSPORT AND ADAPTIVE MESH REFINEMENT: ALGORITHMS AND TESTS OF THE AstroBEAR CODE

ANDREW J. CUNNINGHAM[1], ADAM FRANK[1], PEGGY VARNIÈRE[1,2], SORIN MITRAN[3], AND THOMAS W. JONES[4]

- Solve hyperbolic PDE with elliptic constraints: **MHD**
- Source terms for energy loss/ gain, **ionization dynamics**
- Operator splitting: **gravity, heat conduction** (*HYPRE*)

$$\frac{\partial}{\partial t}\begin{bmatrix}\rho\\ \rho v_x\\ \rho v_y\\ \rho v_z\\ \mathcal{E}\\ B_x\\ B_y\\ B_z\end{bmatrix} + \frac{\partial}{\partial x}\begin{bmatrix}\rho v_x\\ \rho v_x^2 + P + B^2/2 - B_x^2\\ \rho v_y v_x\\ \rho v_z v_x\\ (\mathcal{E} + P + B^2/2)v_x - B_x(\boldsymbol{B}\cdot\boldsymbol{v})\\ 0\\ -E_z\\ E_y\end{bmatrix} +$$

$$\frac{\partial}{\partial y}\begin{bmatrix}\rho v_y\\ \rho v_x v_y\\ \rho v_y^2 + P + B^2/2 - B_y^2\\ \rho v_z v_y\\ (\mathcal{E} + P + B^2/2)v_y - B_y(\boldsymbol{B}\cdot\boldsymbol{v})\\ E_z\\ 0\\ -E_x\end{bmatrix} + \frac{\partial}{\partial z}\begin{bmatrix}\rho v_z\\ \rho v_x v_z\\ \rho v_y v_z\\ \rho v_z^2 + P + B^2/2 - B_z^2\\ (\mathcal{E} + P + B^2/2)v_y - B_z(\boldsymbol{B}\cdot\boldsymbol{v})\\ -E_y\\ E_x\\ 0\end{bmatrix} = \boldsymbol{S}$$

$$\nabla\cdot\boldsymbol{B} = 0.$$

AstroBEAR 2.0
Parallel AMR Performance

Rebuild load balance algorithm across AMR grid hierarchy
(Carroll et al. 2011, in prep.)

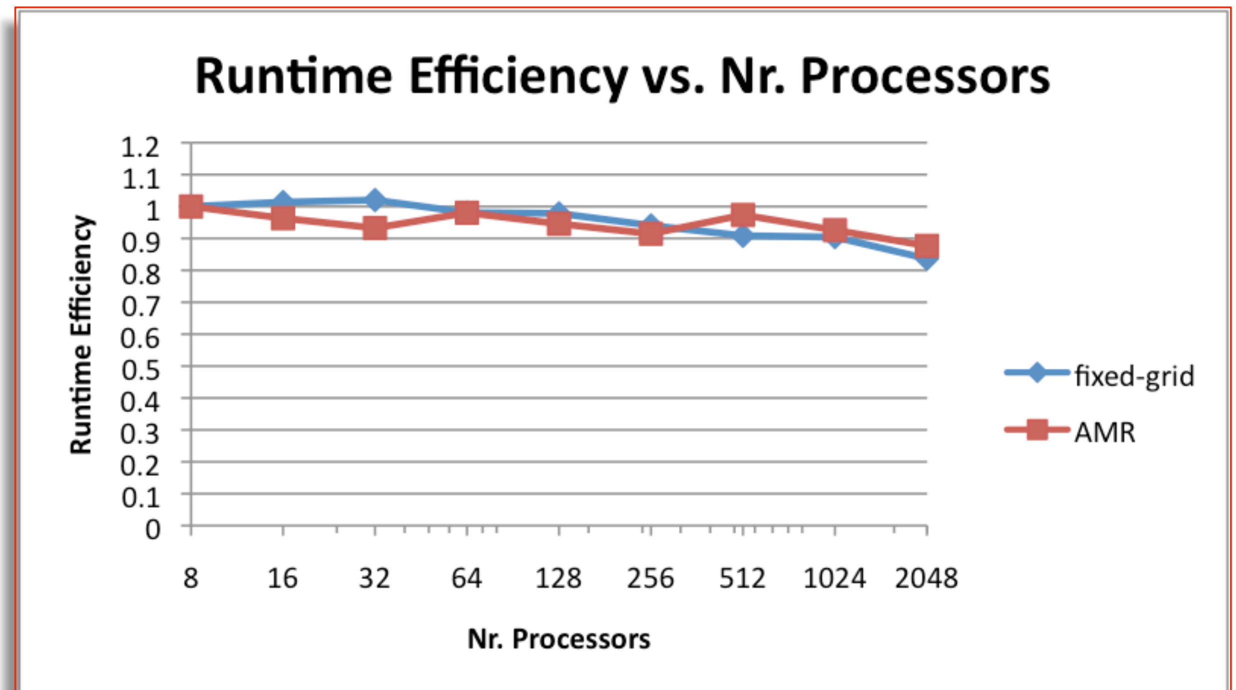

https://clover.pas.rochester.edu/trac/astrobear

Simulations

PFD magnetic tower jet

1. adiabatic
2. cooling
3. adiabatic & rotating

kinetic-energy dominated jet

4. adiabatic
5. cooling
6. adiabatic & rotating

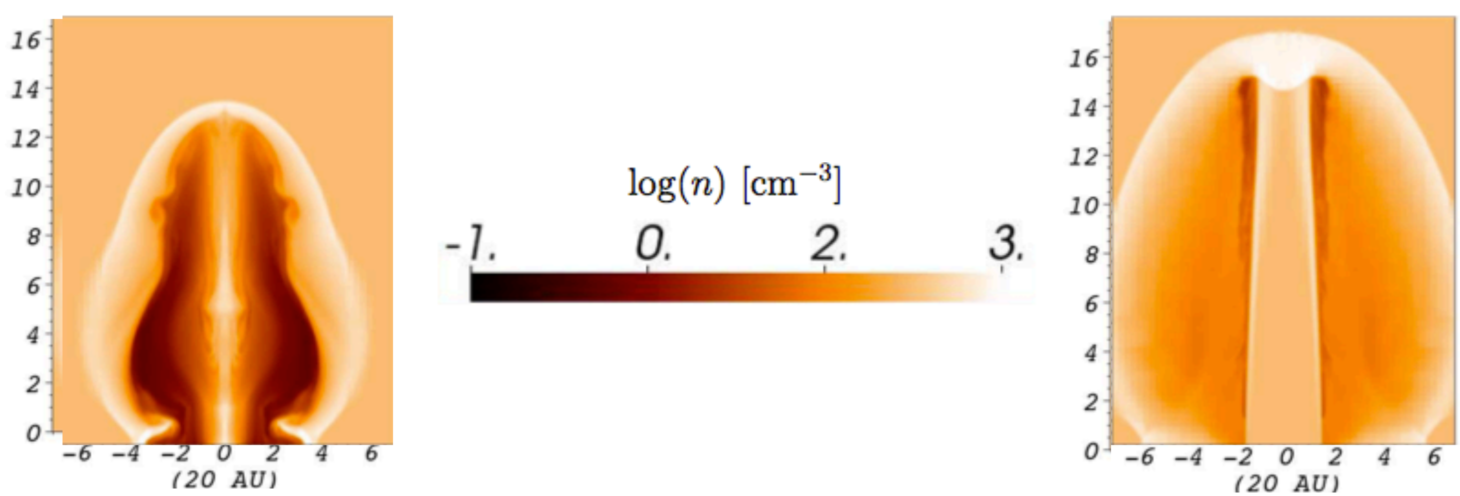

Assumptions

1. **HD jets are collimated** at sub-resolution scales.

2. jets have **same** time averaged max **speed**:

$$v_j = v_z \approx |\mathbf{B}_{\rm max}|(4\,\pi\,\rho^0_{\rm amb})^{-1/2}.$$

3. **Equal injected energy fluxes**:

$$0.5\rho_j v_z^3\, a = (|\mathbf{B}|^2/8\pi)\,(|\mathbf{B}|(4\pi\rho^0_{\rm amb})^{-1/2})\,a,$$

where ρ_j is the jet's density and a (= πr_j^2) is the area of the energy injection region.

Initial conditions

Density = 100 cm^{-3}
Temperature = 10000 K
molecular gas, γ =5/3
V = 0 km s^{-1}.

Magnetic fields **only** within the central region

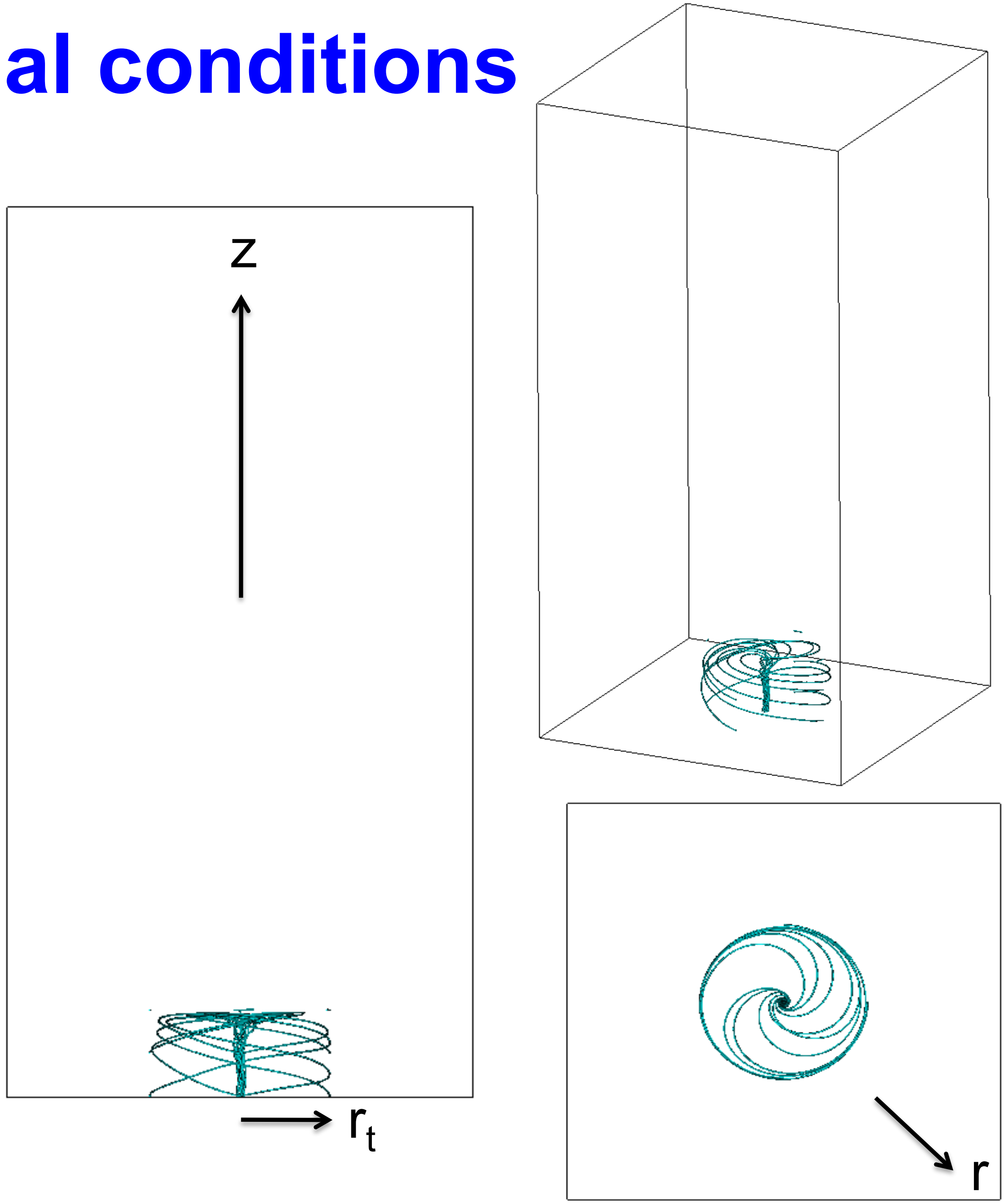

Continuous magnetic energy injection

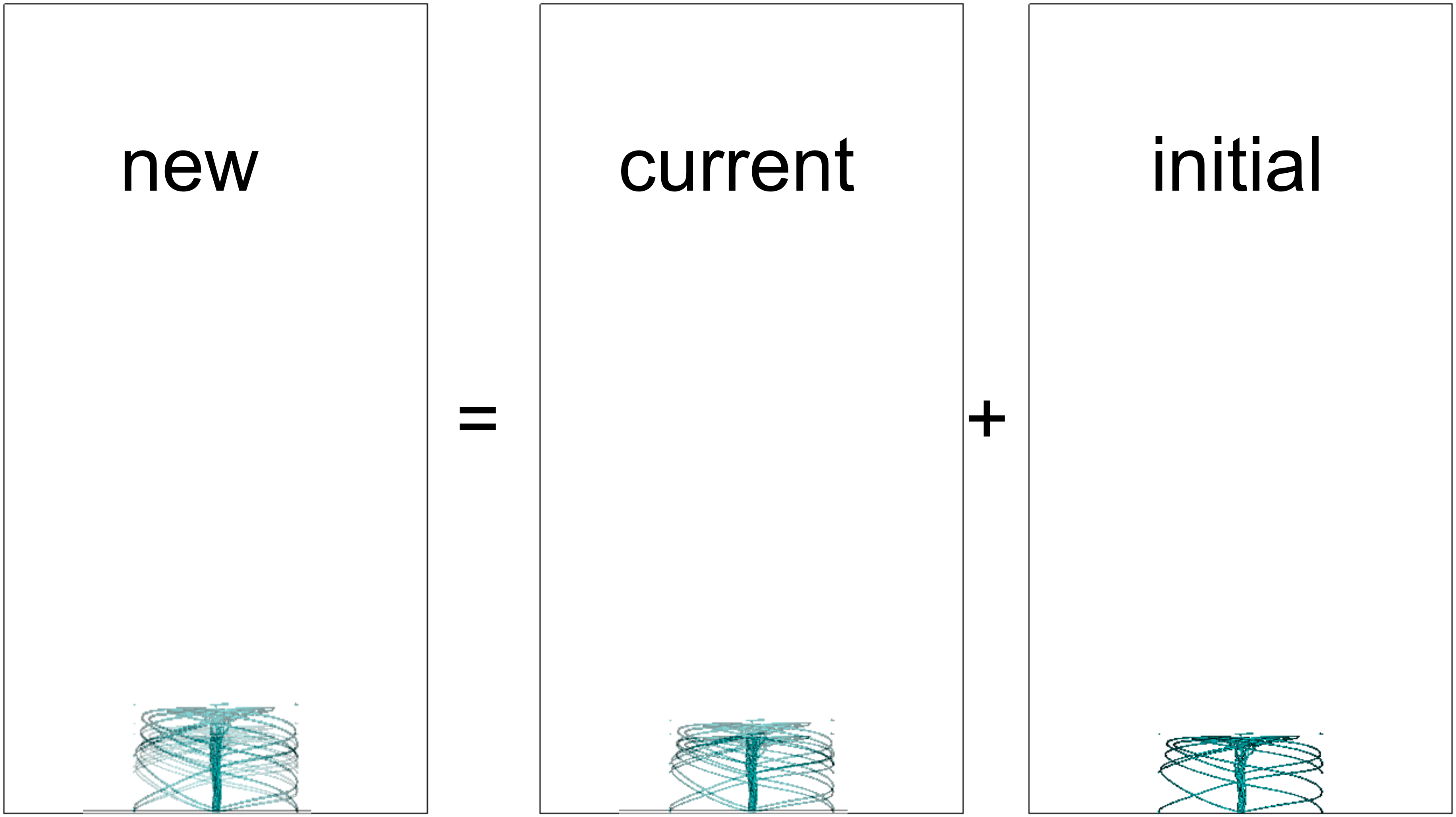

Adiabatic

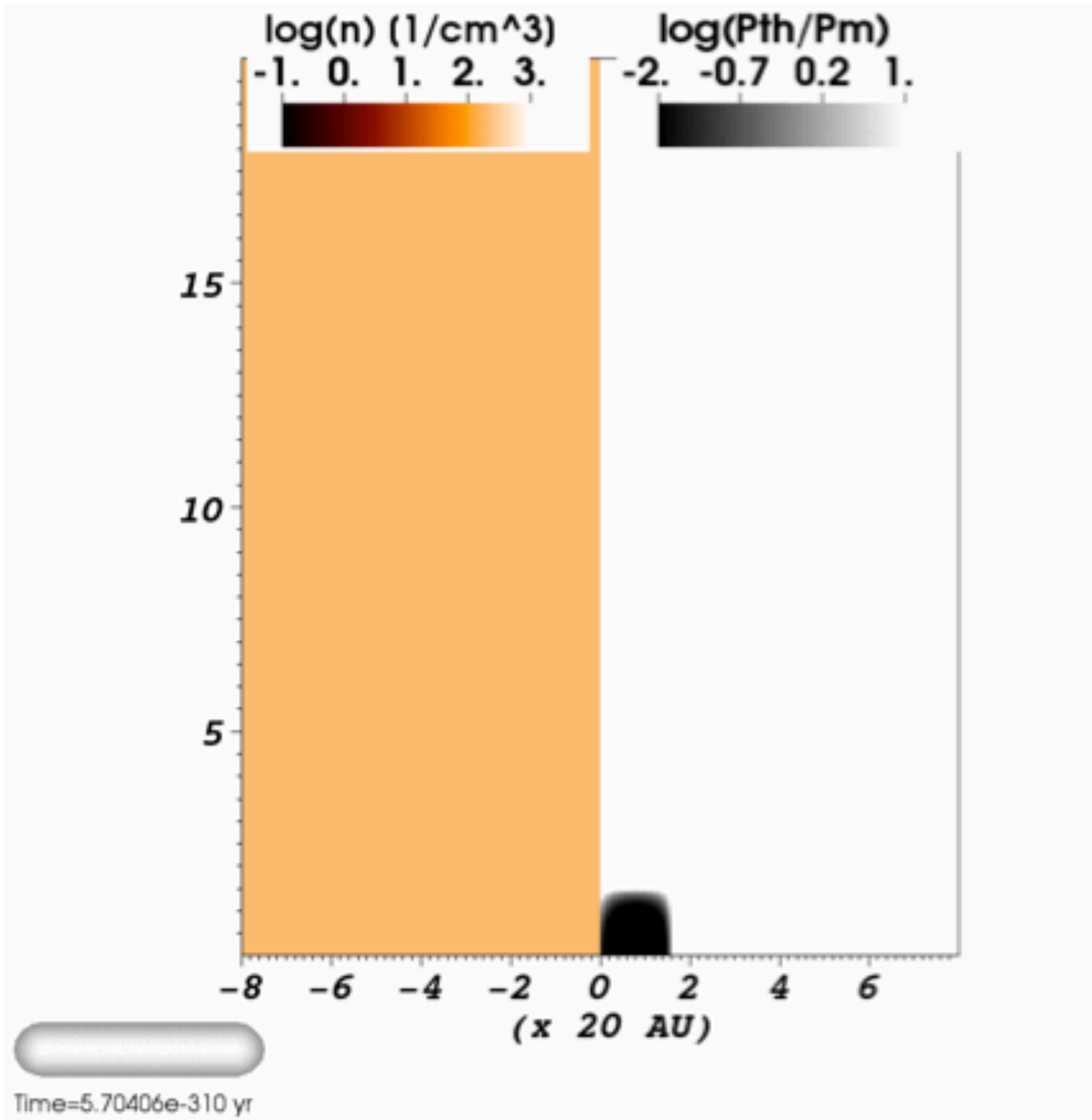

log(n) (1/cm^3)
-1. 0. 1. 2. 3.
log(Pth/Pm)
-2. -0.7 0.2 1.
15
10
5
−8 −6 −4 −2 0 2 4 6
(x 20 AU)
Time=5.70406e-310 yr

Adiabatic

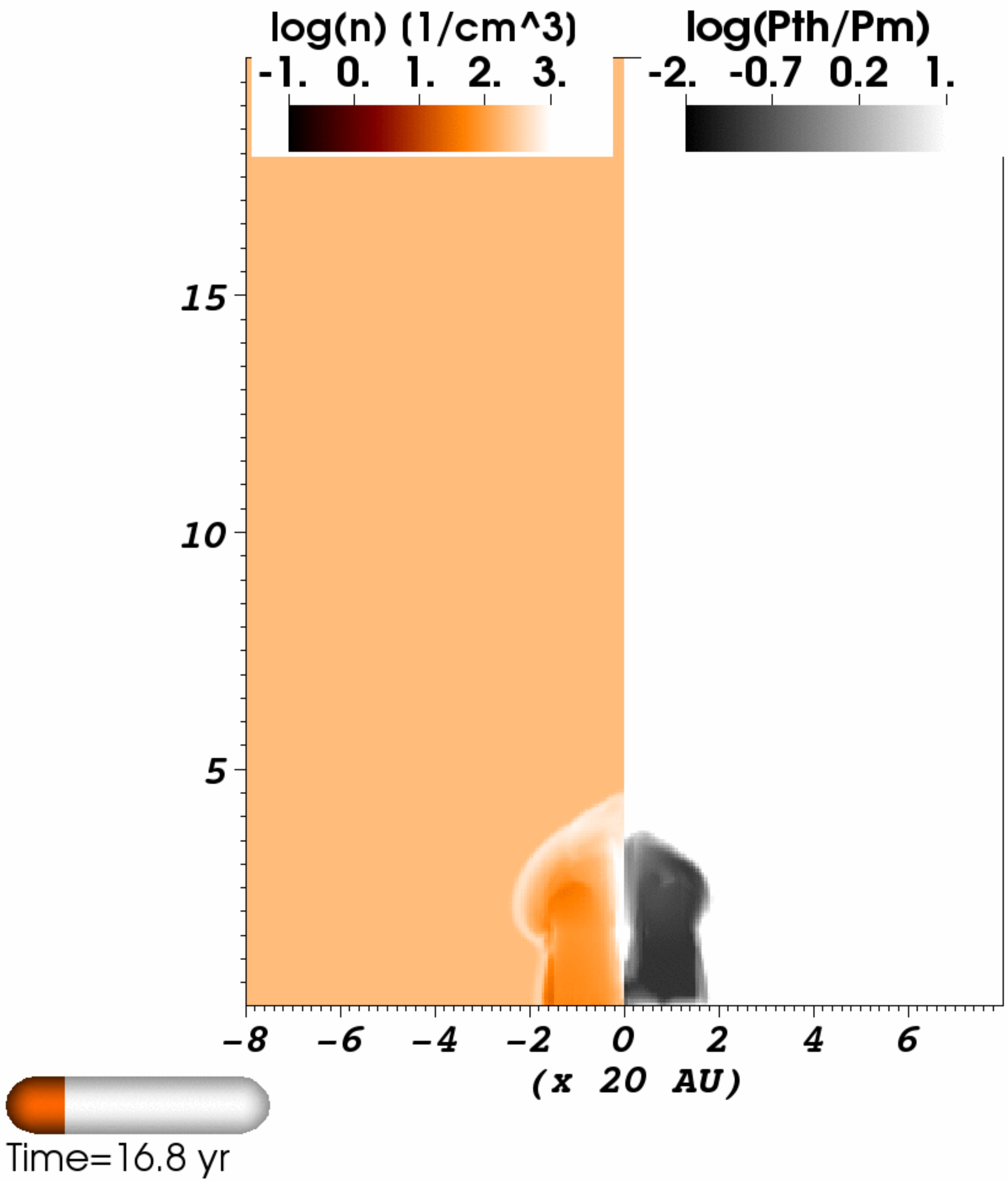

log(n) (1/cm^3)
-1. 0. 1. 2. 3.
log(Pth/Pm)
-2. -0.7 0.2 1.
15
10
5
−8 −6 −4 −2 0 2 4 6
(x 20 AU)
Time=16.8 yr

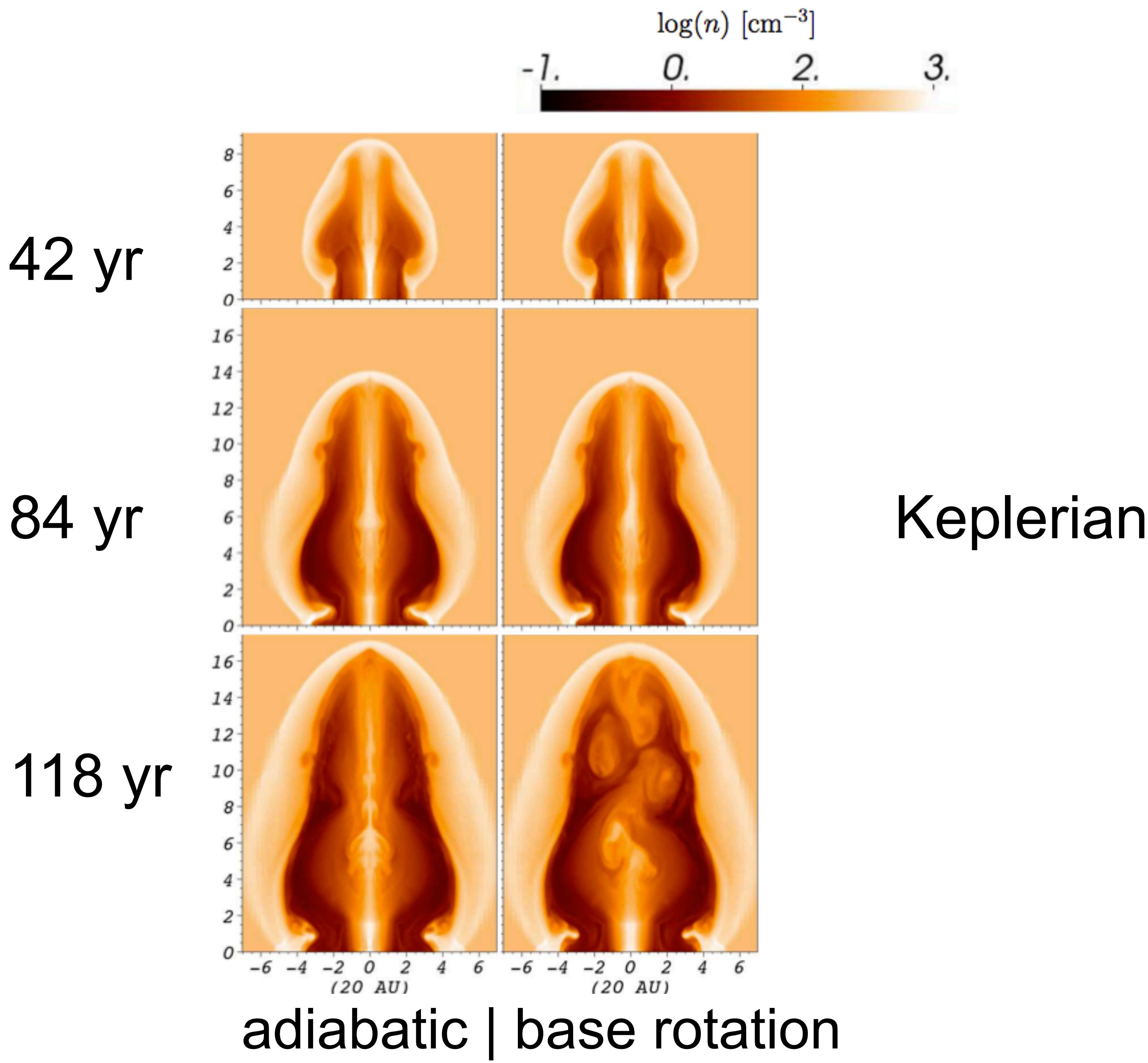
log(n) [cm^-3]
-1.
0.
2.
3.
42 yr
84 yr
118 yr
(20 AU)
(20 AU)
adiabatic | base rotation
Keplerian

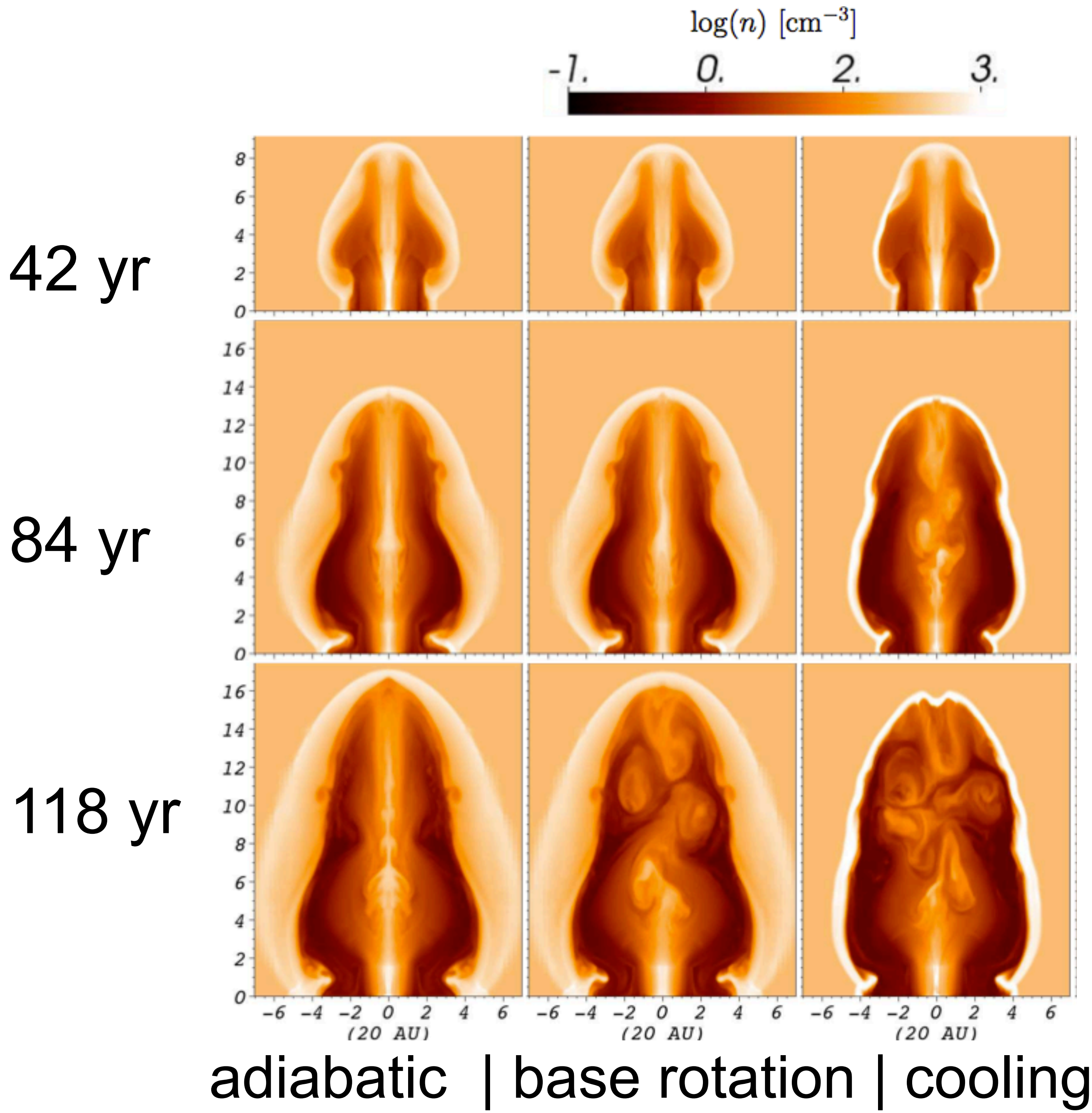

log(n) [cm^-3]
-1.
0.
2.
3.
42 yr
84 yr
118 yr
(20 AU)
adiabatic | base rotation | cooling

Cooling

Dalgarno & Mccray (1972). Ionization of both H and He, the chemistry of H2 and optically thin cooling.

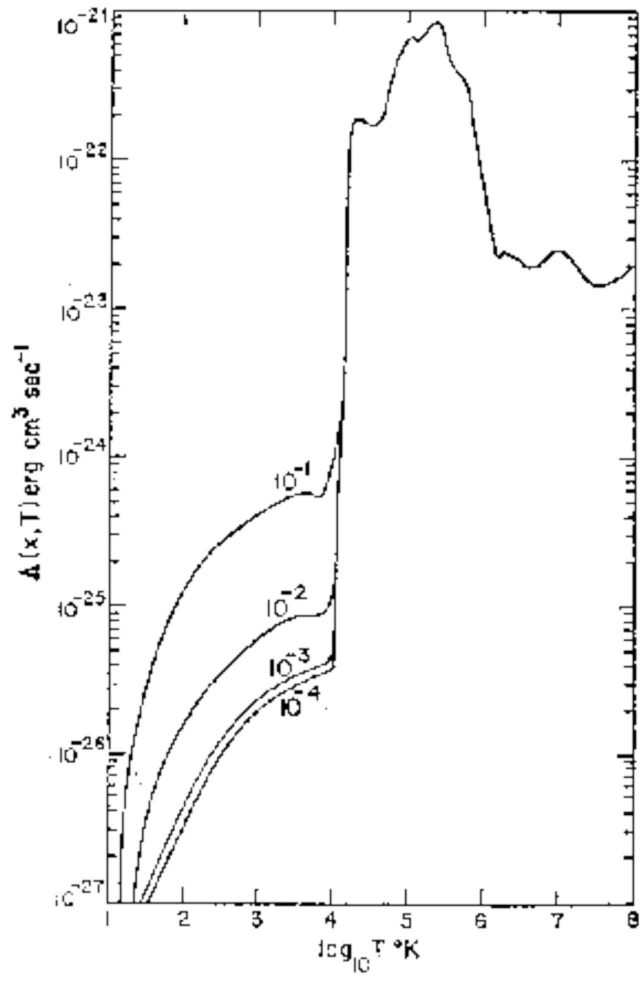

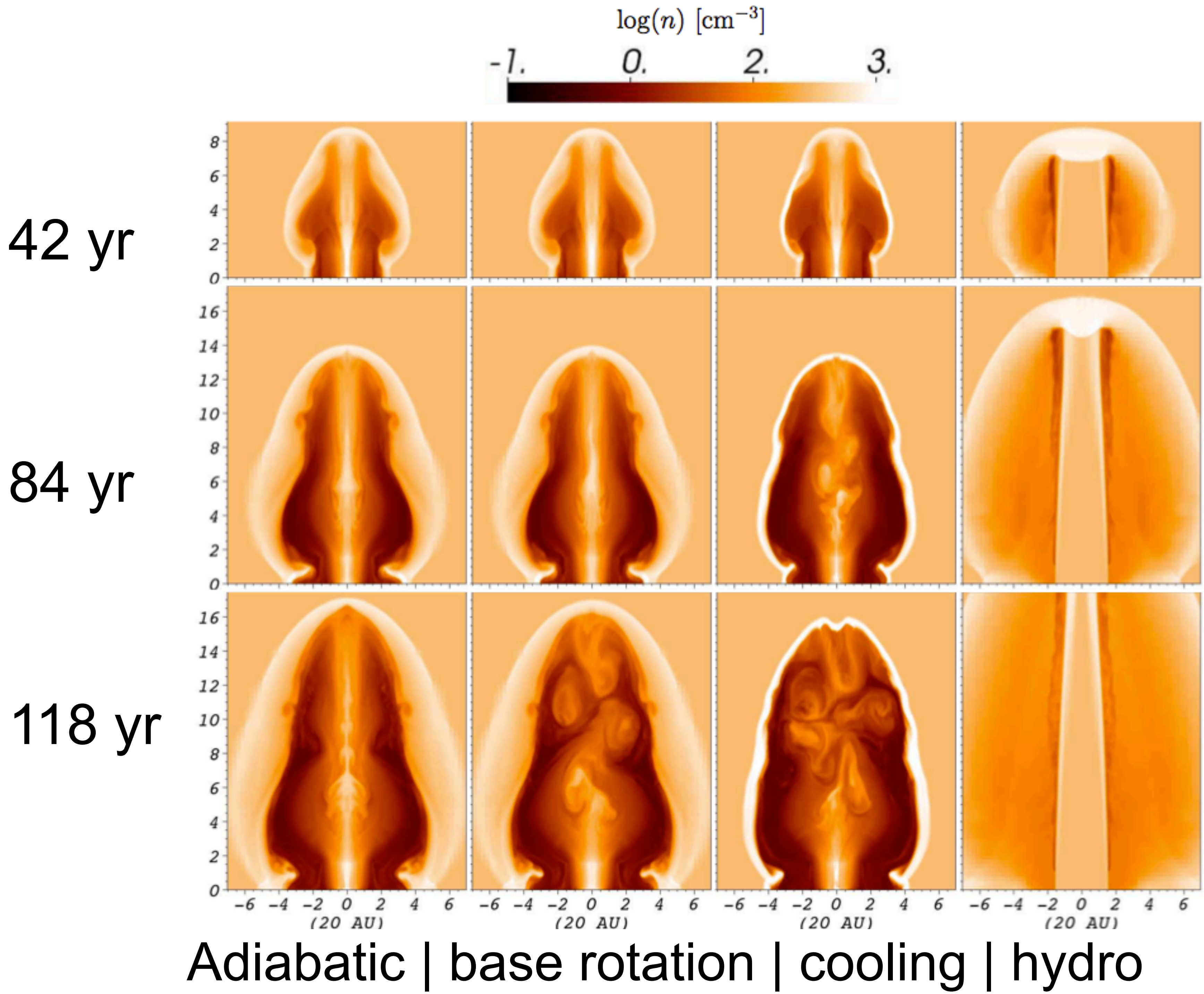

log(n) [cm^-3]
-1.
0.
2.
3.
42 yr
84 yr
118 yr
(20 AU)
Adiabatic | base rotation | cooling | hydro

Field line maps

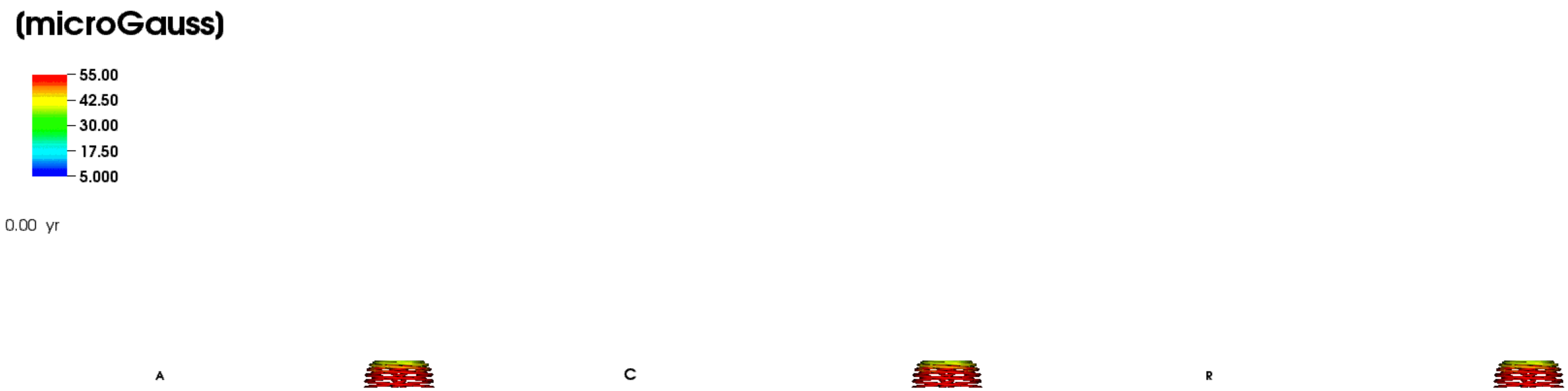

adiabatic cooling base rotation

Only 2 central field lines

Perturbations

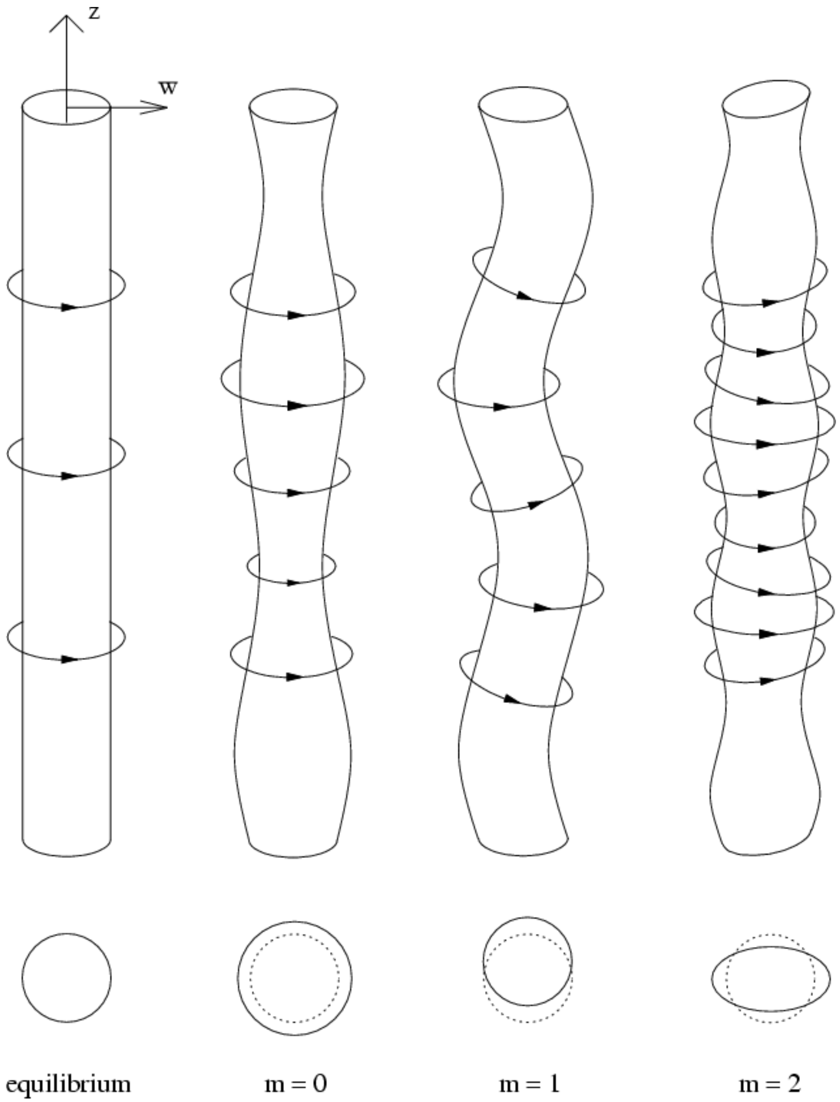

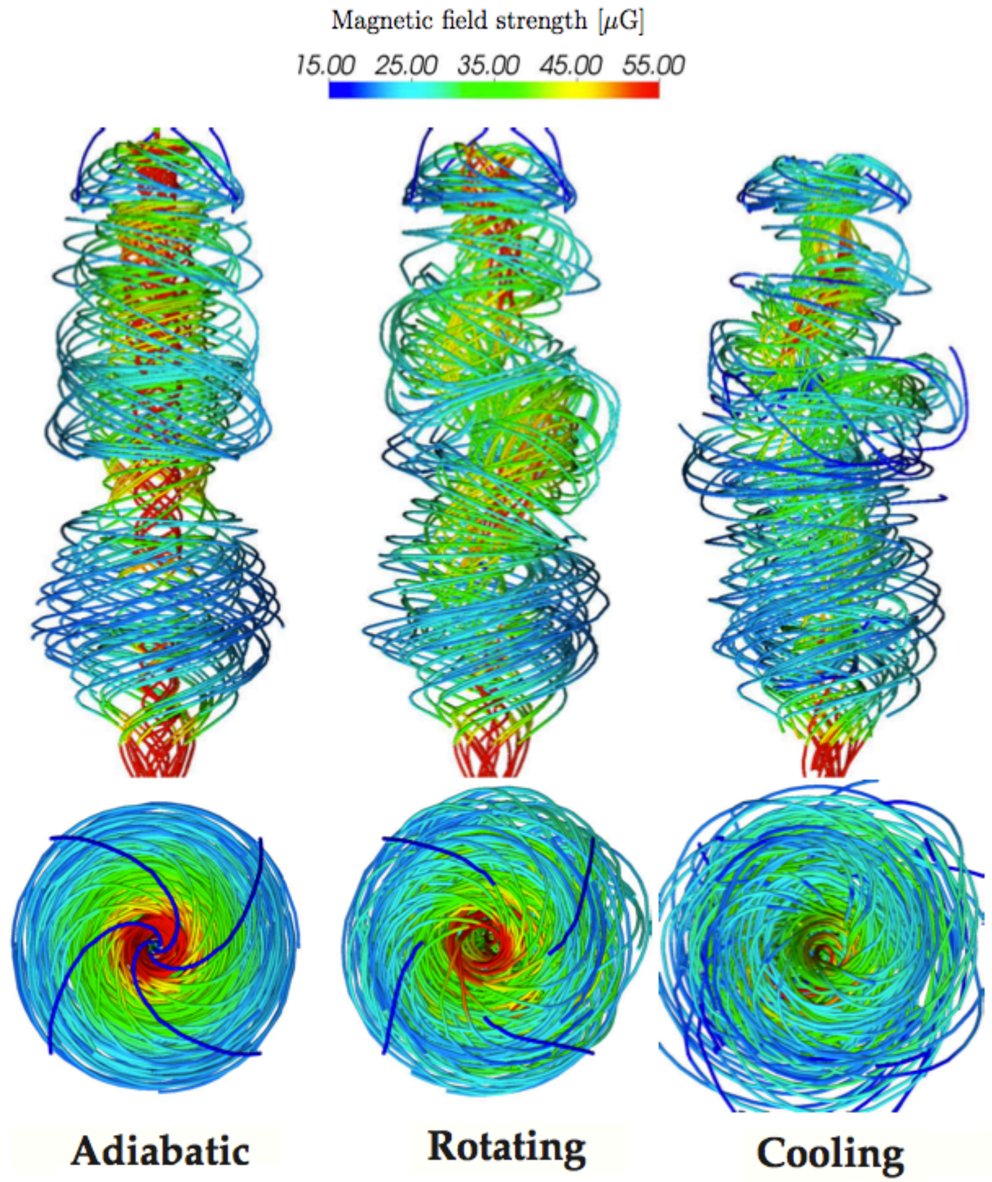

Instability:

$$\left|\frac{B_\phi}{B_z}\right| > |(\beta_z - 1)kr_{jet}|$$

where $\beta_z = 2\mu_0 P/B_z^2$.

Relative strength:

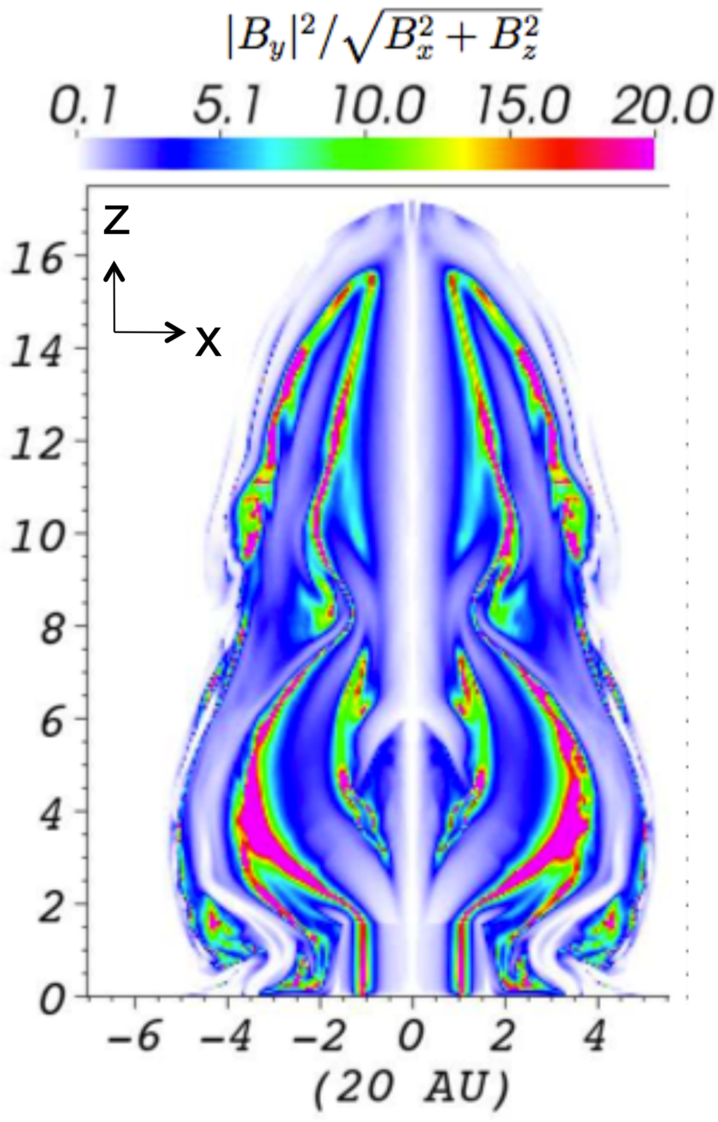

Instability:

$$\left|\frac{B_\phi}{B_z}\right| > |(\beta_z - 1)kr_{jet}|$$

where $\beta_z = 2\mu_0 P/B_z^2$.

Jet velocities:

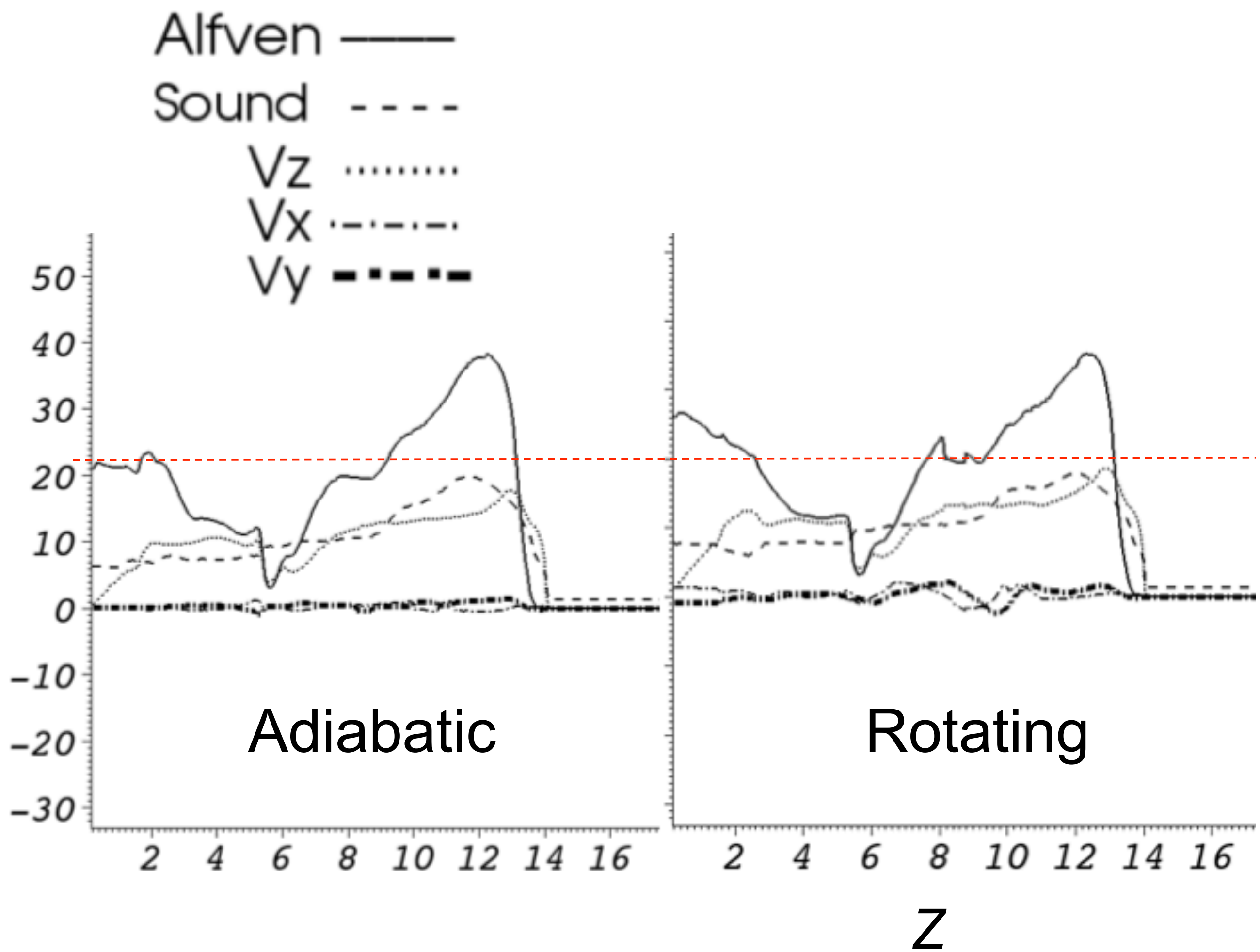

Instability:

$$\left|\frac{B_\phi}{B_z}\right| > |(\beta_z - 1)kr_{jet}|$$

where $\beta_z = 2\mu_0 P/B_z^2$.

Jet velocities:

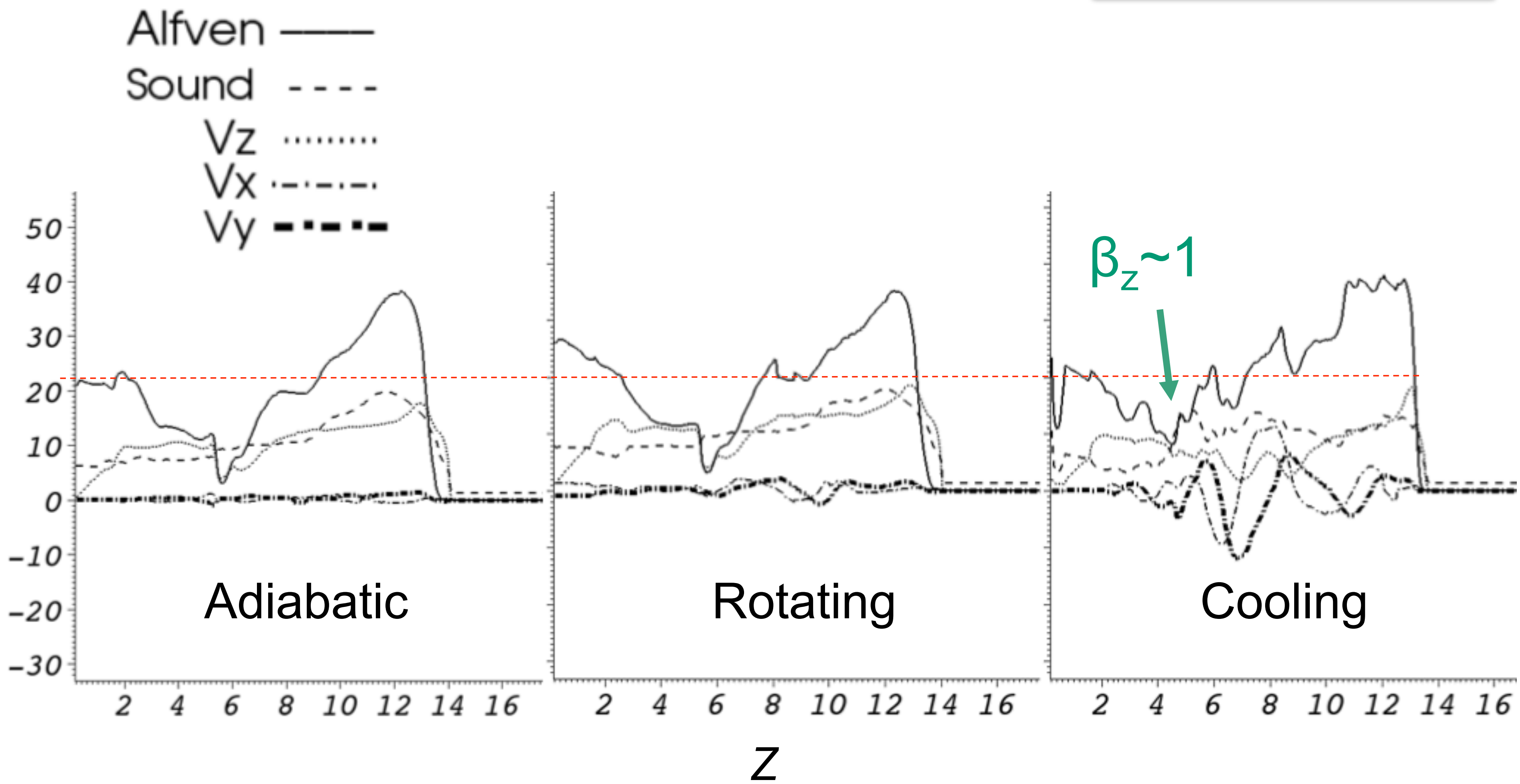

Beam energy flux

Cooling case (but rotating is similar)

Poynting

$$f_P = \int_s [\mathbf{B} \times (\mathbf{V} \times \mathbf{B})]_z \, dS,$$

Kinetic

$$f_k = \int_s \frac{1}{2} \rho |\mathbf{V}|^2 V_z \, dS.$$

$$\log|Q(\mathbf{x},t)| = \log\left|\frac{f_P}{f_k}\right|$$

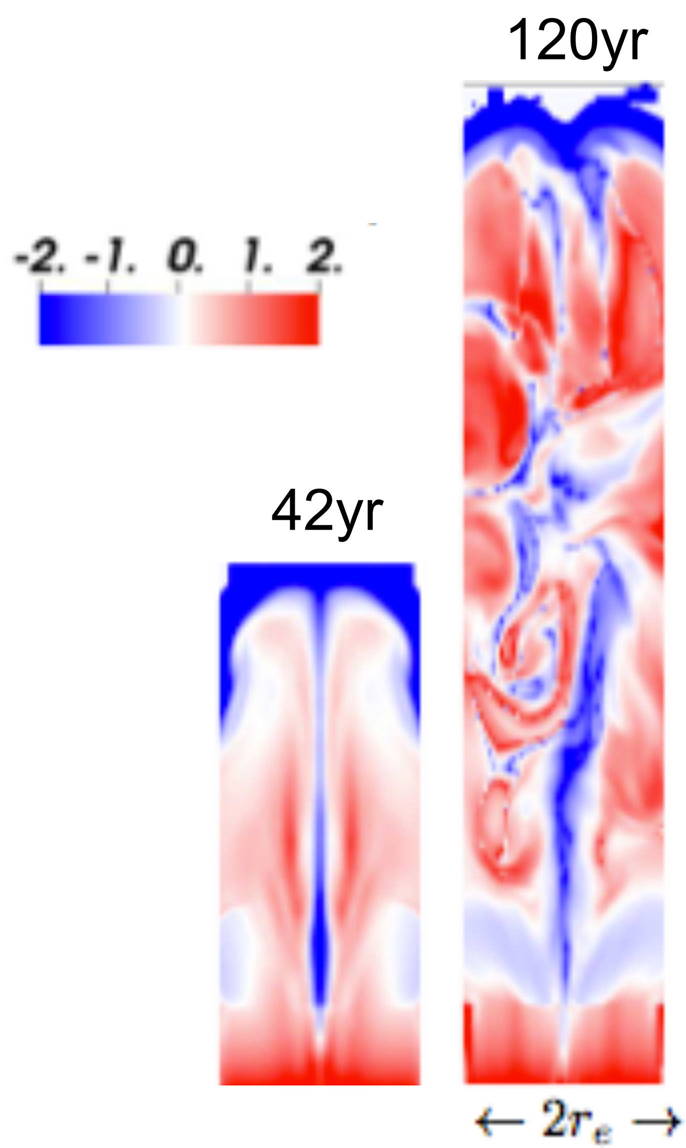

¿Preguntas?

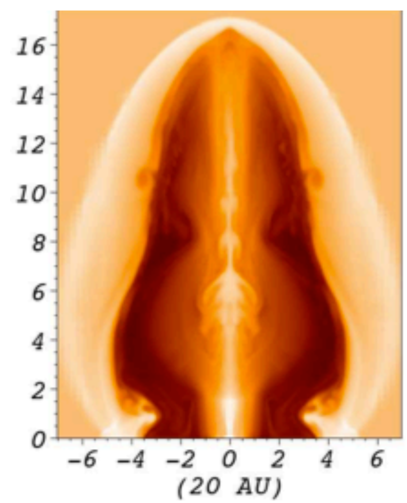

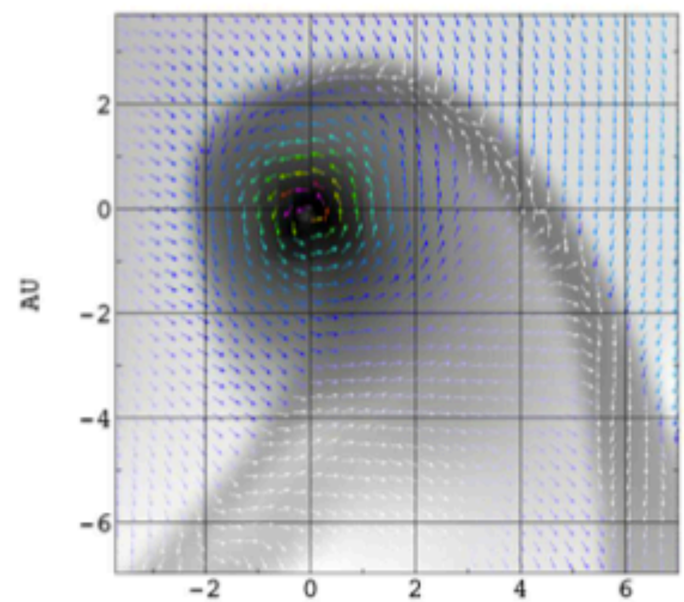

Disks in common envelope binaries

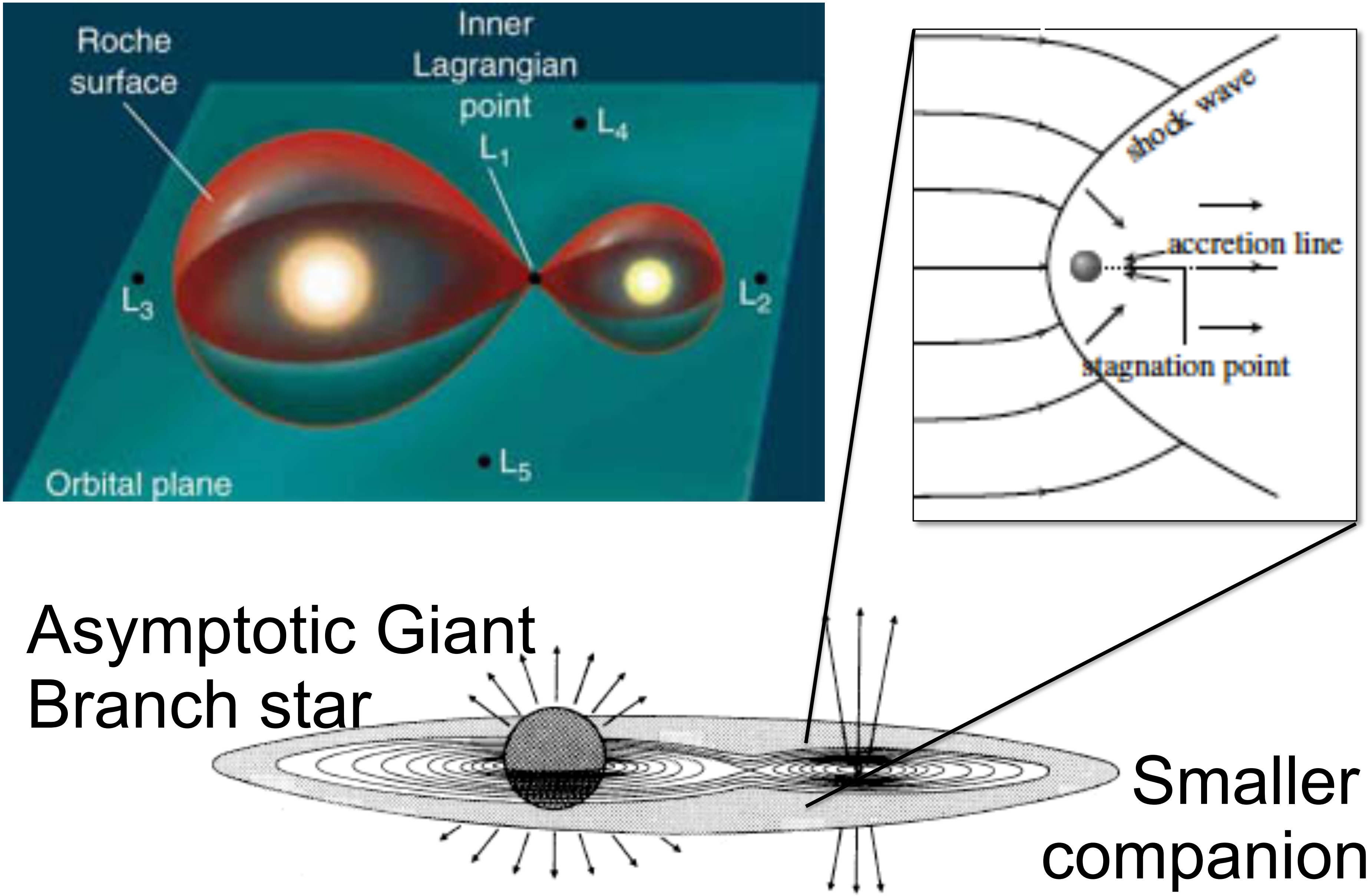

Physics: Wind Accretion in Binaries

Old question: Few numerical studies

1. What is limit of disk accretion?
   a = 20 AU, 30 AU, 40 AU?

2. What is the accretion rate?
   = Bondi-Hoyle
   > Bondi-Hoyle
   < Bondi-Hoyle

$$R_a = 2GM_2/v_r^2$$

Bondi-Hoyle Accretion

Disk Formation Condition in Planetry Nebulae

(Soker & Rapport 2000)

$$\frac{J_a}{J_c} = f\left(\frac{M_{AGB} + M_c}{1.2M_\Theta}\right)^{1/2}\left(\frac{M_c}{0.6M_\Theta}\right)^{3/2}\left(\frac{R_c}{.01R_\Theta}\right)^{-1/2}\left(\frac{a}{10au}\right)^{-3/2}\left(\frac{V_r}{15km/s}\right)^{-4}$$

where:

J_a and J_c are the specific angular momenta of the accreted material and that of a particle in Keplerian orbit at the equator of an accreting star of radius R_c, respectively

a is the distance between the center of the stars; the separation

V_r is the relative velocity of the wind and the accretor.

Previous numerical studies

The Astrophysical Journal, 497:303–329, 1998 April 10

BIPOLAR PREPLANETARY NEBULAE: HYDRODYNAMICS OF DUSTY WINDS IN BINARY SYSTEMS. I. FORMATION OF ACCRETION DISKS

Nikos Mastrodemos and Mark Morris

Model: 3D, **SPH**, dusty wind models, accretion disks formation about the binary companion to the mass-losing giant of asymmetric PN.

Free parameters: wind velocity, binary separation and rotation of the mass-loosing star

Results: Stable thin accretion disks form around the companion. Their equilibrium structure has elliptical streamlines with a range of eccentricities. Such disks may be **susceptible to tilt or warping instabilities**. Wind accretion in such binaries is stable, displaying no evidence for any type of flip-flop instability.

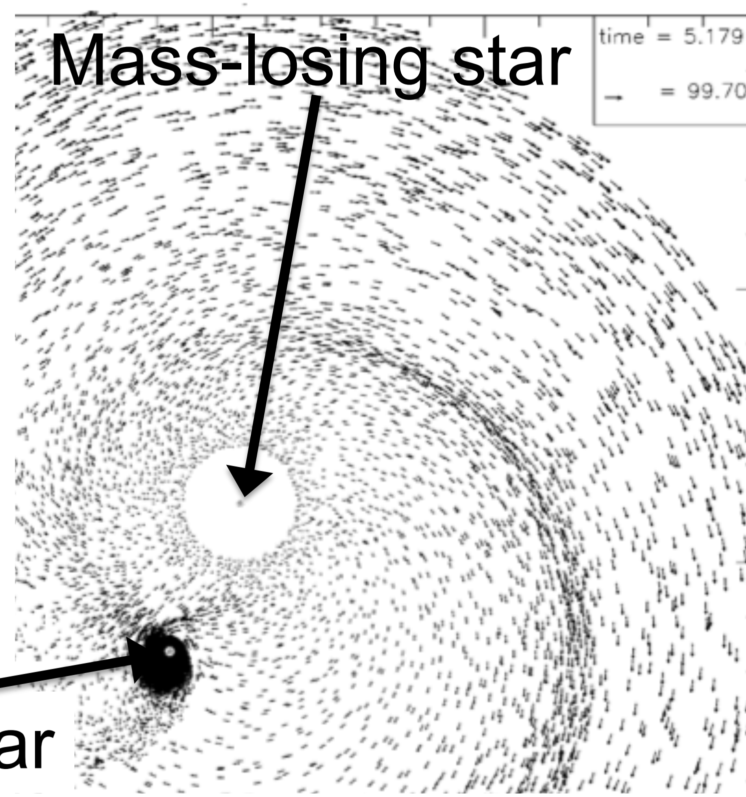

The Astrophysical Journal, 700:1148–1160, 2009 August 1 doi:10.1088/0004-637X/700/2/1148

NUMERICAL SIMULATIONS OF WIND ACCRETION IN SYMBIOTIC BINARIES

M. de Val-Borro[1], M. Karovska, and D. Sasselov

Model: symbiotic binaries, **2D**, no self-gravity, large separations, relevant for Mira AB (Karovska et al. 2005).

Free parameters: mass-loss rate, wind temperature depends on the distance from the mass losing star and its companion, orbital separation.

Results: Flow pattern similar to **a Roche lobe overflow** with accretion rates of 10% of the mass loss from the primary**. Stable Keplerian thin disks,** exponential density profiles, $M \sim 10^{-4} M_{sun}$. Tidal streams and disks form and show a dependence with AGB mass loss. The evolution of **the binary system**, and its independent components, is **affected by mass transfer** through focused winds.

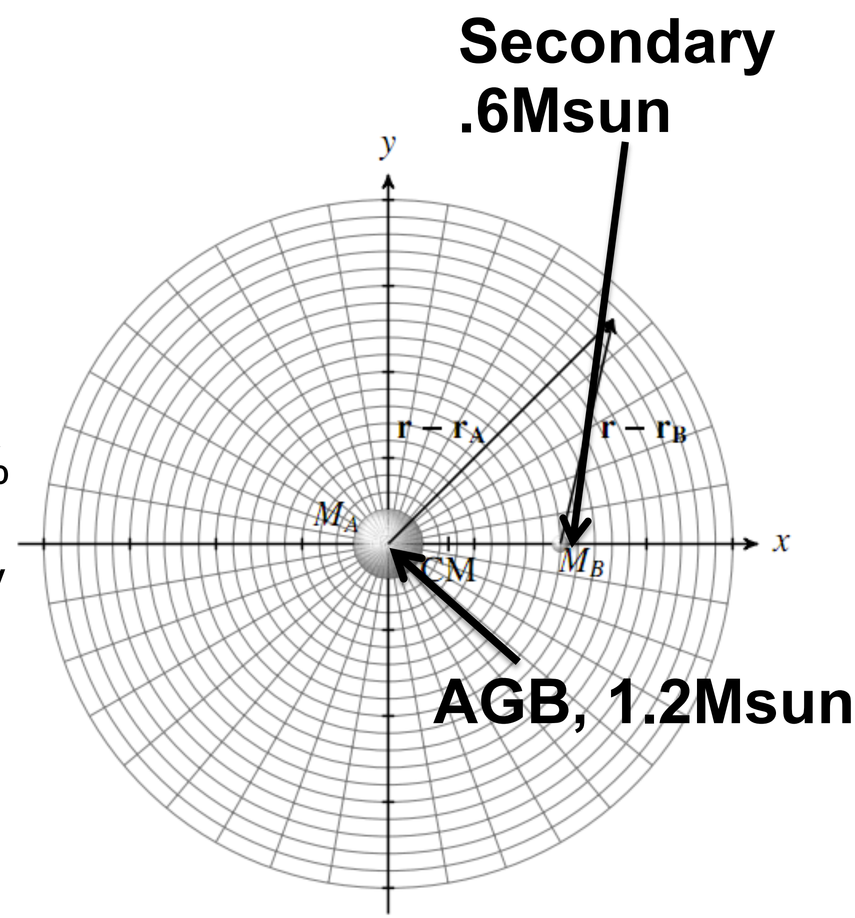

Figure 7. Schematic representation of the grid geometry in the polar coordinates. The physical quantities are defined in the center of the cells. The system is centered on the primary and rotating in clockwise direction.

The wind is accelerated at 10, 20, 30, and 40 AU, from left to right.

Orbital period

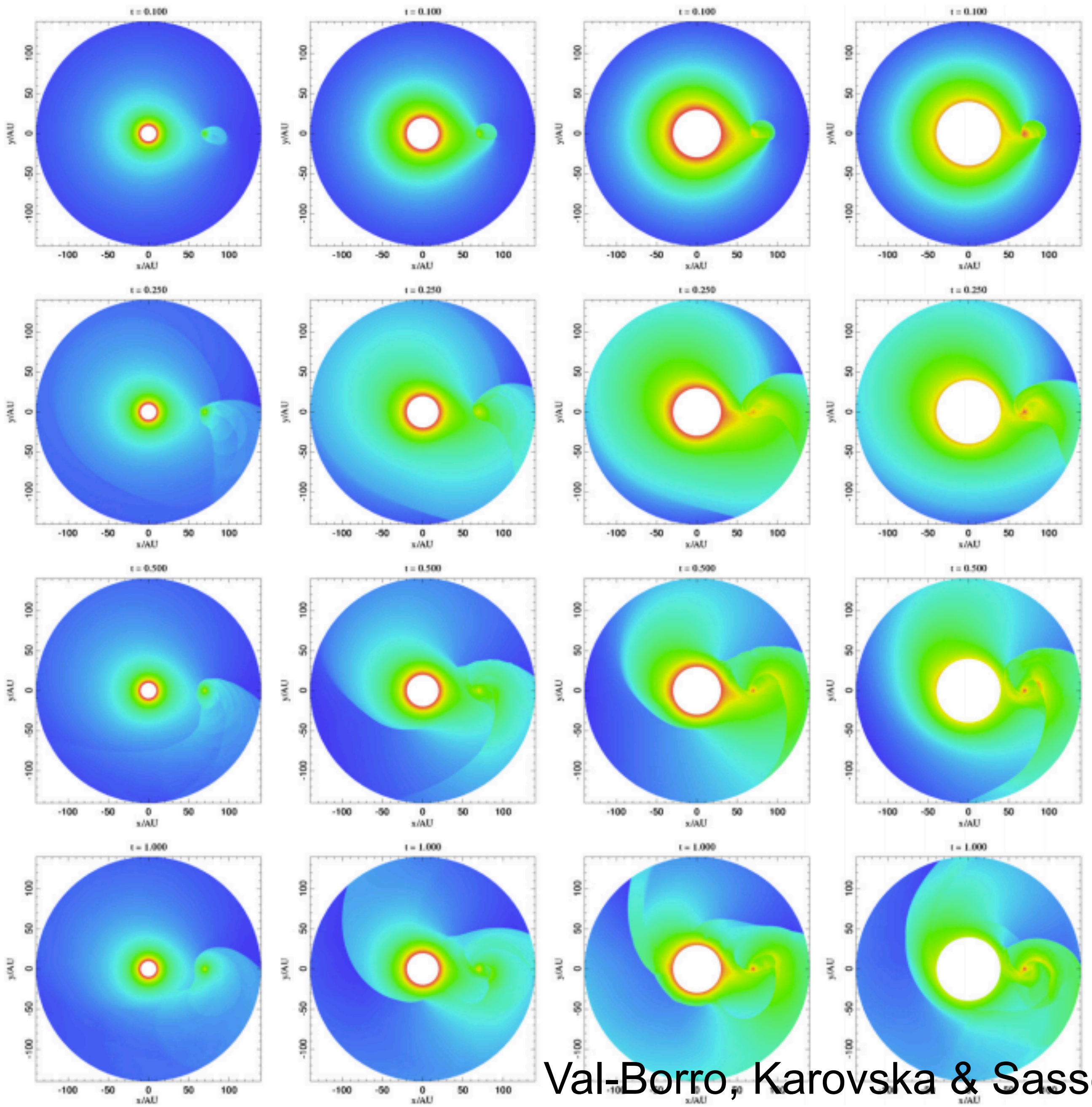

Val-Borro, Karovska & Sasselov, 2009

Our model: Huarte-Espinosa et al. 2012b, in prep.

Grid and initial conditions

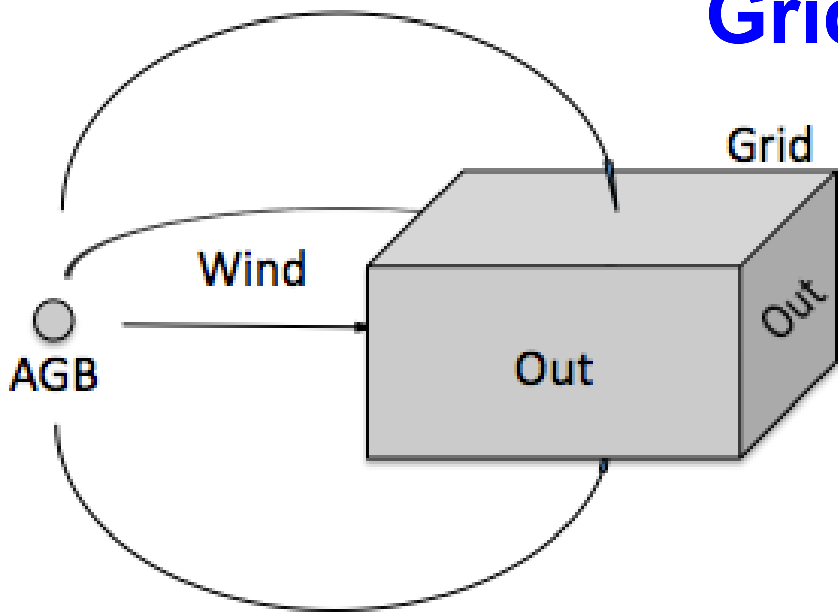

- Co-rotating frame of reference, nested grid
- Circular orbits

- Primary: AGB with spherical wind (v=10km/s, mass-loss($r_{injection}$)~$10^{-5}M_{sun}$/yr) and M_1=1.5M_{sun}
- Secondary: accretor with M_2=M_{sun}
- Separations =10,15,20AU
- γ=1.001; isothermal (like M&M '98)

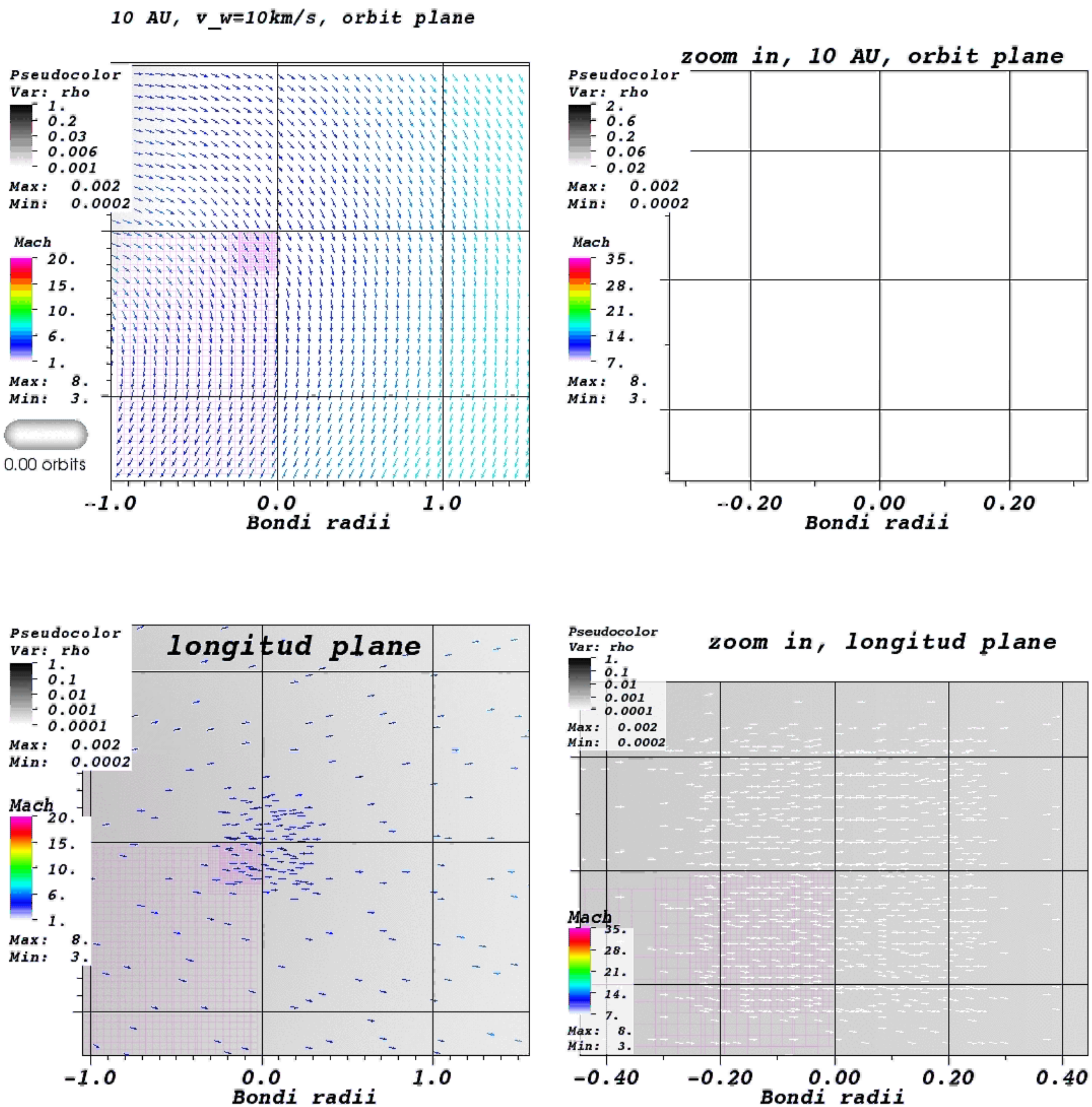
10 AU, v_w=10km/s, orbit plane
Pseudocolor
Var: rho
1.
0.2
0.03
0.006
0.001
Max: 0.002
Min: 0.0002
Mach
20.
15.
10.
6.
1.
Max: 8.
Min: 3.
0.00 orbits
-1.0
0.0
1.0
Bondi radii
zoom in, 10 AU, orbit plane
Pseudocolor
Var: rho
2.
0.6
0.2
0.06
0.02
Max: 0.002
Min: 0.0002
Mach
35.
28.
21.
14.
7.
Max: 8.
Min: 3.
-0.20
0.00
0.20
Bondi radii
longitud plane
Pseudocolor
Var: rho
1.
0.1
0.01
0.001
0.0001
Max: 0.002
Min: 0.0002
Mach
20.
15.
10.
6.
1.
Max: 8.
Min: 3.
-1.0
0.0
1.0
Bondi radii
zoom in, longitud plane
Pseudocolor
Var: rho
1.
0.1
0.01
0.001
0.0001
Max: 0.002
Min: 0.0002
Mach
35.
28.
21.
14.
7.
Max: 8.
Min: 3.
-0.40
-0.20
0.00
0.20
0.40
Bondi radii

Disk structure

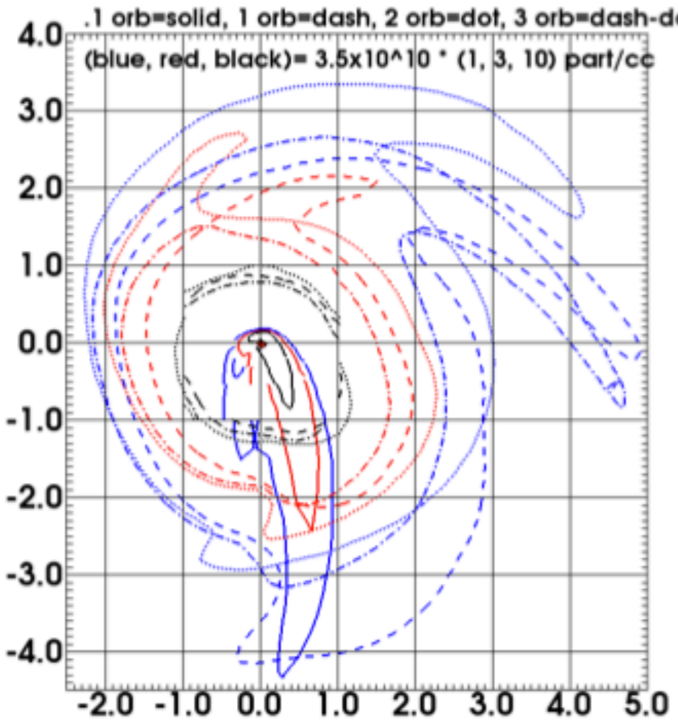

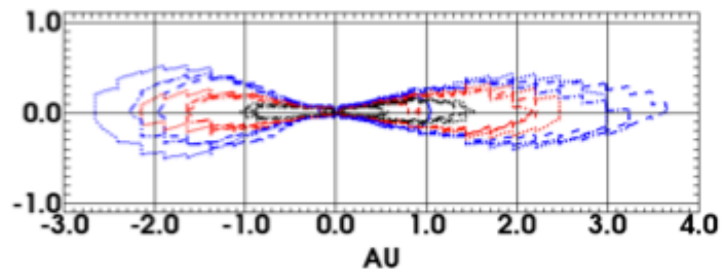

a=10 AU

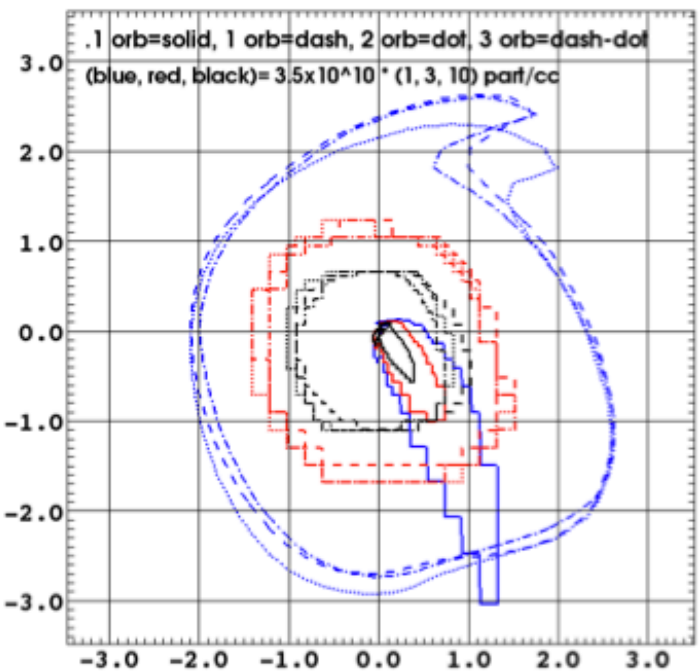

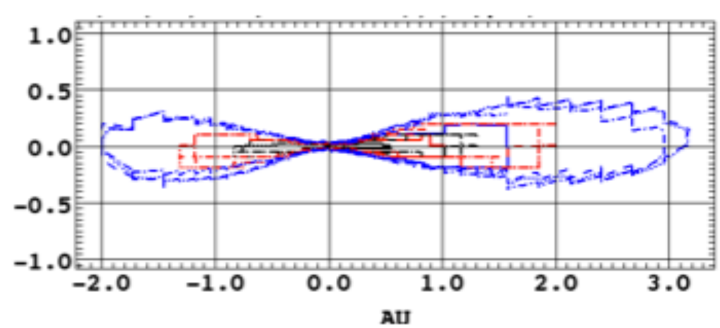

a=15 AU

Disk structure

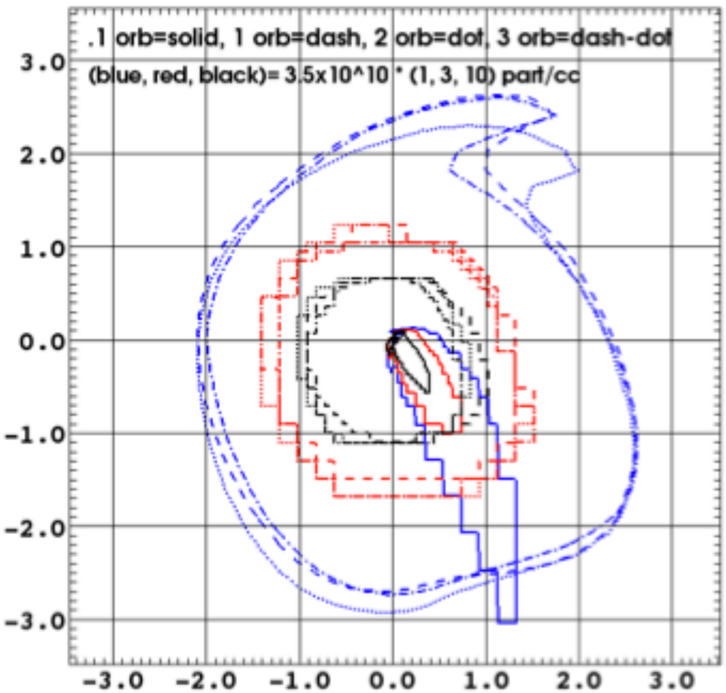

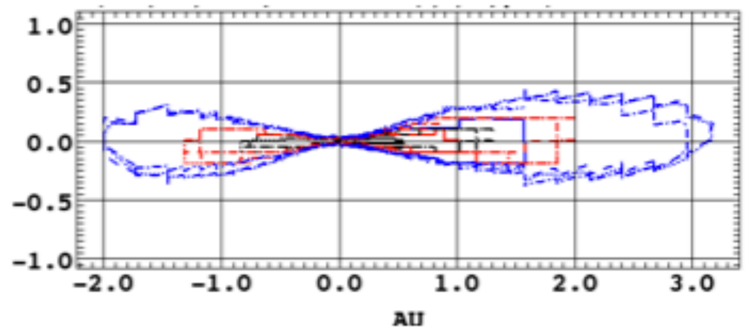

a=15 AU

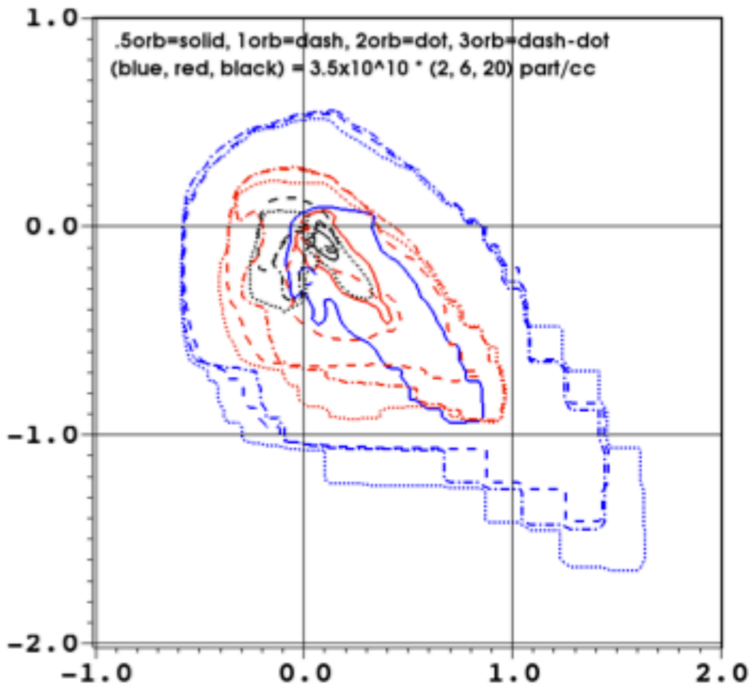

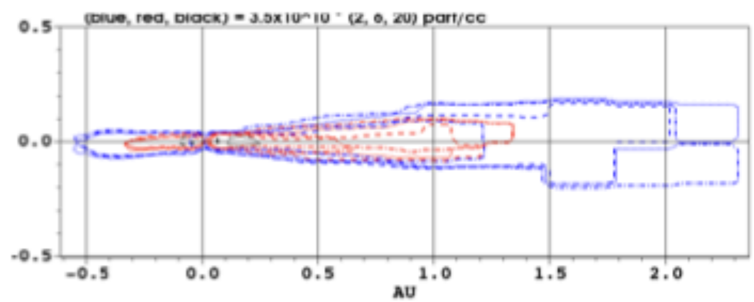

a=20 AU

Accretion rate onto the secondary

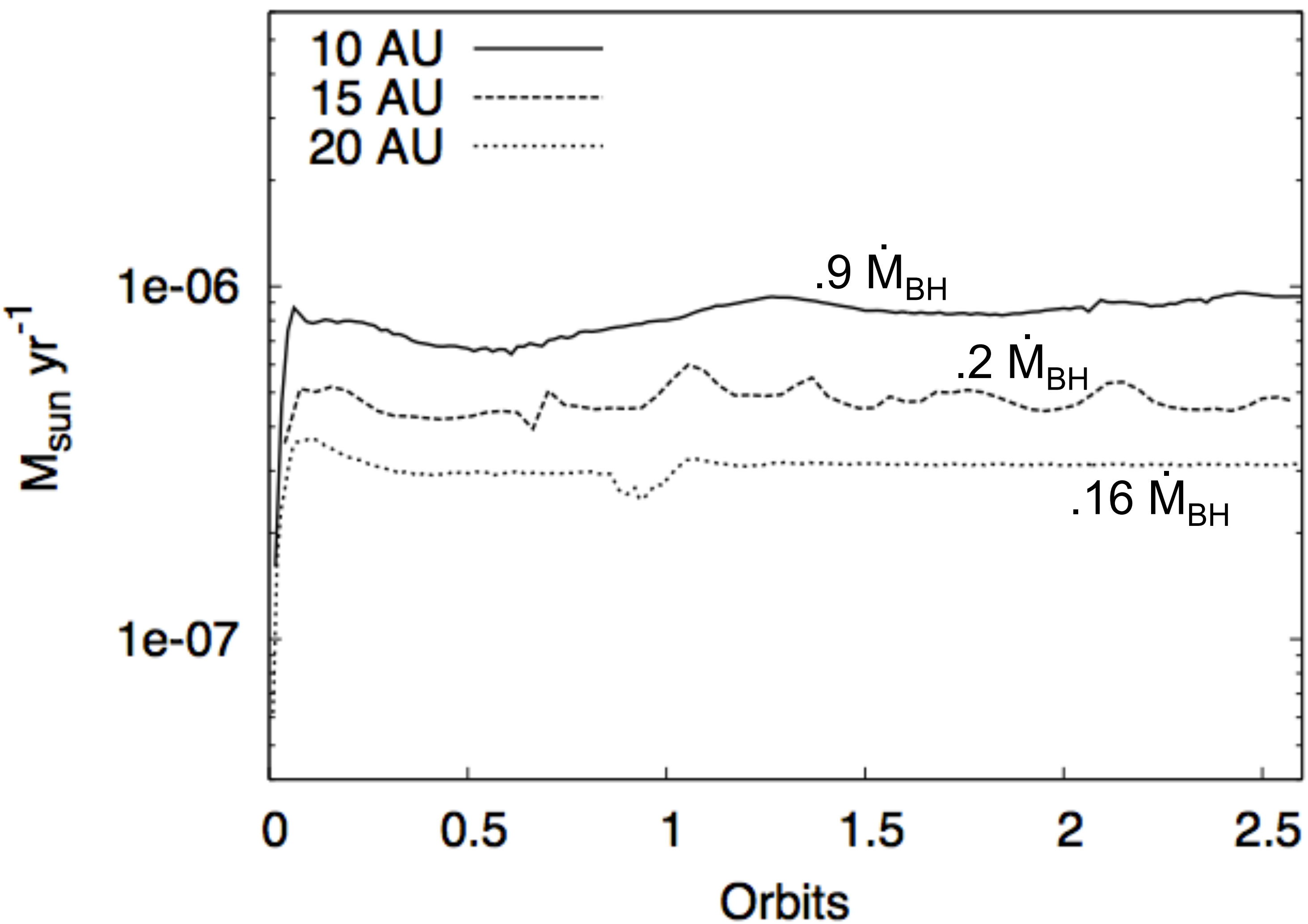

Disk orbits depend on the binary separation

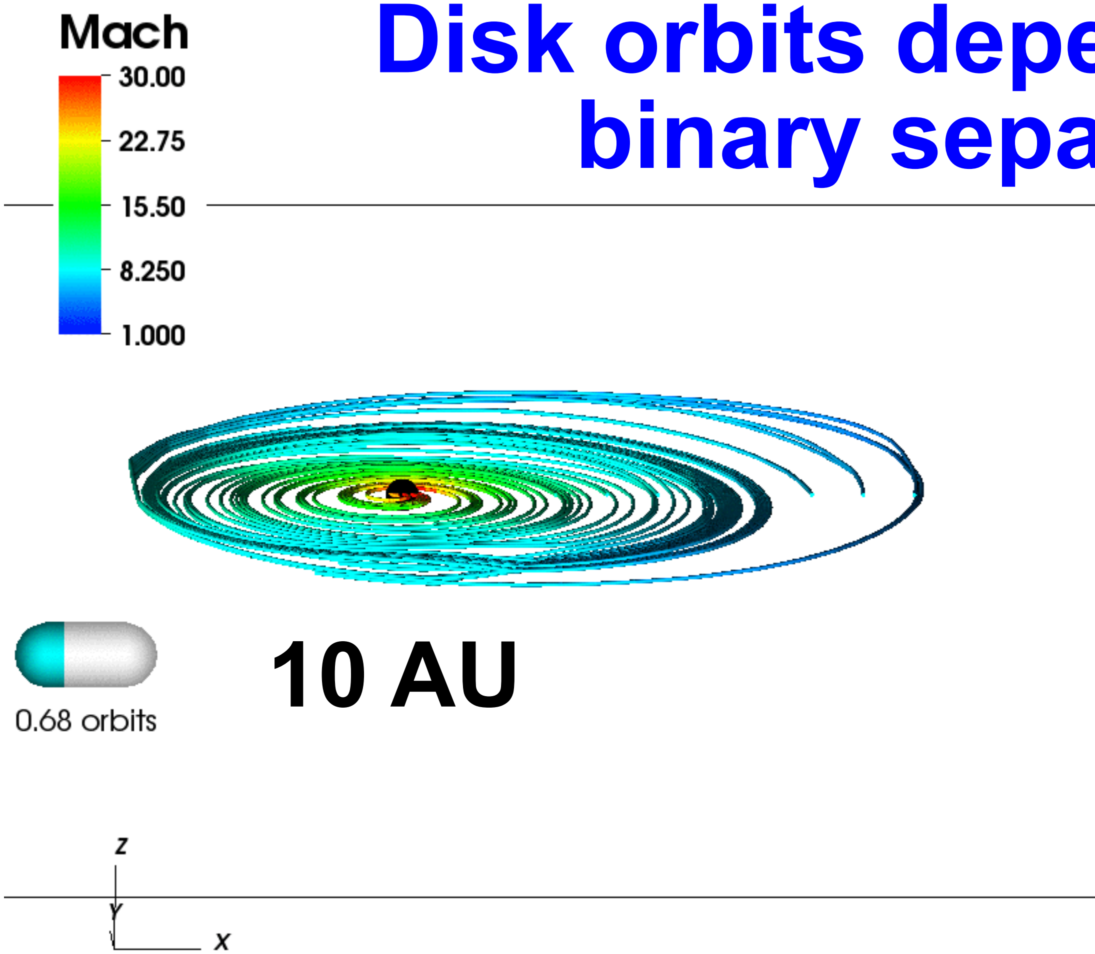

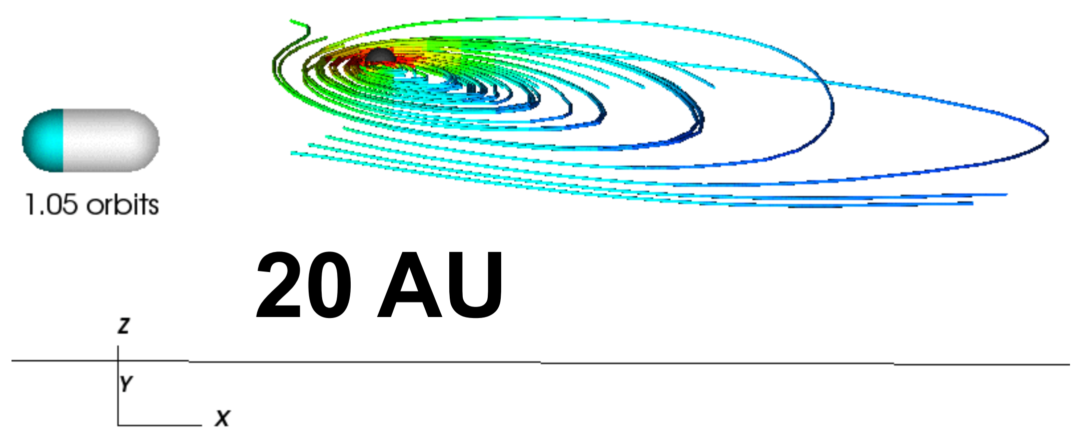

Summary
Jets

-PFD jets more unstable and structurally different than purely HD jets with same energy flux.

-Base rotation amplifies B_φ exacerbating a pressure unbalance and leading to kink instability.

-Cooling reduces the thermal energy of the core and r_{jet} thus it's insufficient to damp magnetic pressure kink perturbations.

-PFD jet beams eventually yield a series of collimated clumps which may then evolve into kinetic-energy dominated jets at large distances from the engine. Relevant for YSO and possibly other jets too.

-Our model towers agree with MAGPIE lab experiments, even though no tuning was made. I.e. robust results which reveal generic properties of PFD outflows.

Summary
Disks

- The disks' radii and height are inversely proportional to *a,*

- We see disks forming up to 20 AU in 3D,

- Disks' material orbits are a function of *a,*

- The resolution of the impact parameter is key to follow the formation of disks in these kind of models,

- $\dot{M}_{secondary}$ form our models are insufficient to account for the launch of jets in post-AGB stars (pre-PN; see Blackman & Nordhaus, 2007, who have estimated jet mass losses ~ 5×10^{-4} $M_\odot$ yr^{-1}).

Summary
Disks

- The disks' rad

- We see disks

- Disks' materia

- The resolution of the impact parameter is key in these kind of models to follow the formation of disks

¡Gracias!

Encuentra esta plática en: http://www.pas.rochester.edu/~martinhe/talks.html

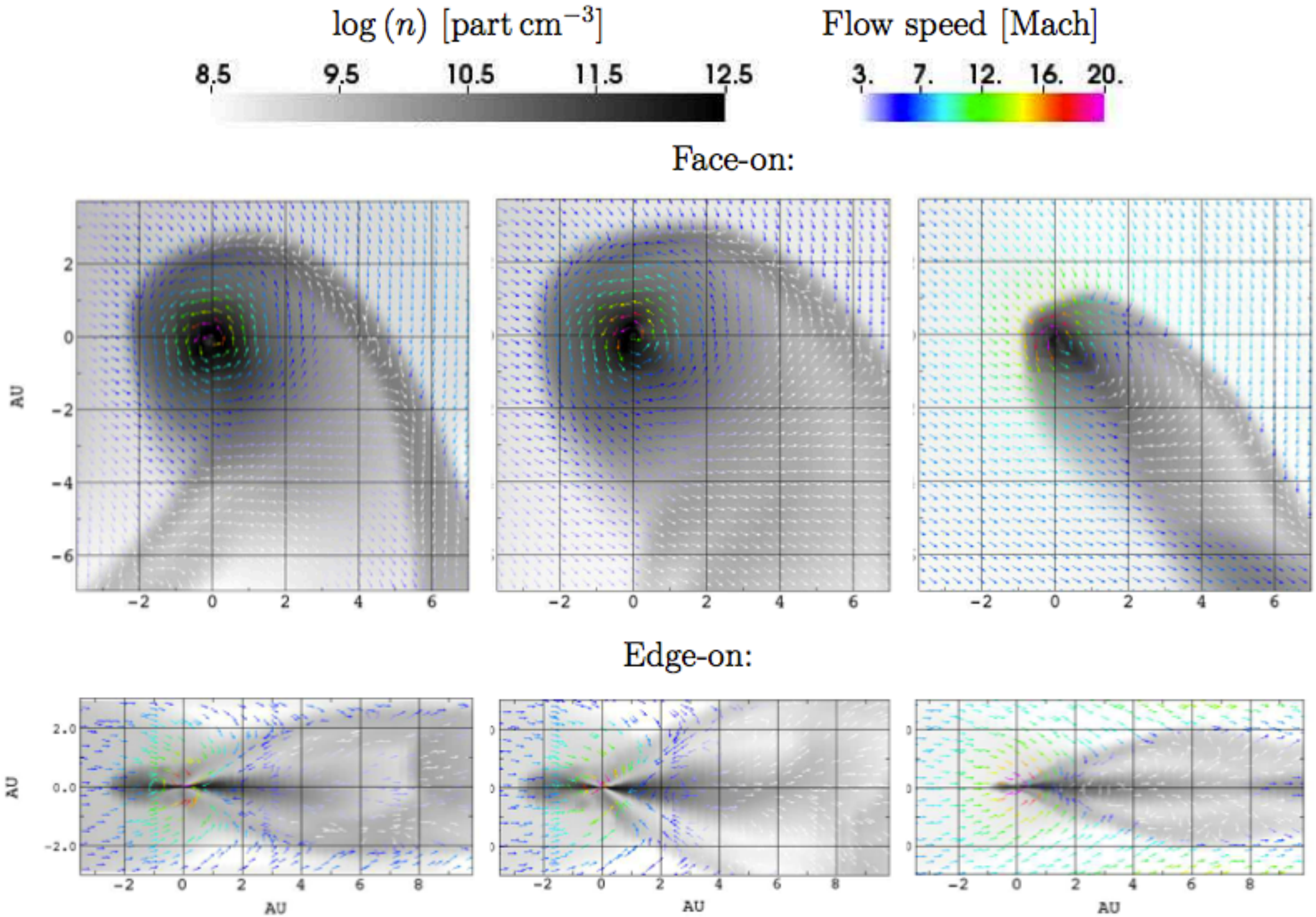

log (n) [part cm^-3]
8.5
9.5
10.5
11.5
12.5
Flow speed [Mach]
3.
7.
12.
16.
20.
Face-on:
Edge-on:
AU